DISTRIBUTION AGREEMENT

In presenting this thesis or dissertation as a partial fulfillment of the requirements for an advanced degree from Emory University, I hereby grant to Emory University and its agents the non-exclusive license to archive, make accessible, and display my thesis or dissertation in whole or in part in all forms of media, now or hereafter known, including display on the world wide web. I understand that I may select some access restrictions as part of the online submission of this thesis or dissertation. I retain all ownership rights to the copyright of the thesis or dissertation. I also retain the right to use in future works (such as articles or books) all or part of this thesis or dissertation.

_____

Ranjith Babu

The Efficacy and Endocytosis of uPAR-targeted Quantum Dots

By

Ranjith Babu

Master of Science

Biology

_____
Lily Yang, MD Ph.D.
Adviser

_____
Darrell Stokes, Ph.D.
Committee Member

_____
Robert Liu, Ph.D.
Committee Member

Accepted:

_____

Lisa A. Tedesco, Ph.D.
Dean of the Graduate School

_____
Date

The Efficacy and Endocytosis of uPAR-targeted Quantum Dots

By

Ranjith Babu

Adviser: Lily Yang, MD Ph.D.

An Abstract of
A thesis submitted to the Faculty of the Graduate
School of Emory University in partial fulfillment
of the requirements for the degree of
Master of Science
In
Biology

2009

ABSTRACT

The Efficacy and Endocytosis of uPAR-targeted Quantum Dots
By Ranjith Babu

Nanoparticles offer a wide variety of functionalities for both the treatment and imaging of cancer. One method of increasing efficiency is by coupling nanoparticles with ligands that target receptors that are overexpressed on cancer cells. One such receptor is the urokinase plasminogen activator receptor (uPAR). The urokinase plasminogen activator (uPA), which is a serine protease, binds to uPAR through its amino terminal fragment (ATF). This portion of the protein has been sequenced, allowing for its production and purification. This peptide can then be conjugated to nanoparticles, allowing them to target cancer cells that overexpress uPAR.

The efficacy of uPAR-targeted nanoparticles in comparison to a free chemotherapeutic agent was investigated using spectroscopy, biomass assays and fluorescence microscopy. It was seen that there was a 3-4 fold increase in the number of targeted nanoparticles within cells compared to their untargeted counterparts. These targeted particles were also more effective in killing cells than the free chemotherapeutic drug. Next, whether uPAR-targeted nanoparticles entered cells via a caveolae-mediated endocytotic mechanism was investigated using caveolin-1 knockout cells. It was seen that there was approximately 50% fewer nanoparticles in caveolin-1 knockout cells compared to the wild-type. The results also showed that uPAR-targeted nanoparticles were not as efficacious in caveolin-1 knockout cells. These results demonstrated that caveolin-1 plays a significant role in uPAR-mediated endocytosis. However, as targeted particles still accumulated within caveolin-1 knockout cells, there are alternate mechanisms by which this can occur.

The Efficacy and Endocytosis of uPAR-targeted Quantum Dots

By

Ranjith Babu

Adviser: Lily Yang, MD, Ph.D.

A thesis submitted to the Faculty of the Graduate
School of Emory University in partial fulfillment
of the requirements for the degree of
Master of Science
In
Biology

2009

TABLE OF CONTENTS

List of Figures

INTRODUCTION

1.1 Cancer and Nanomedicine

Cancer is one of the major causes of mortality in the United States, and is increasing in incidence worldwide. Cancer has resulted in the deaths of approximately 7.6 million people worldwide in 2007, and is the second leading global killer, accounting for 12.5% of all deaths (Larocque, Bharali, & Mousa, 2009). Also, the World Health Organization estimates that cancer will become the greatest cause of death worldwide by the year 2010 (Larocque et al., 2009). Despite its continued devastating impact on human life worldwide, progress is being made in developing more effective treatments to counter this lethal disease.

Current treatments include a combination of surgery, chemotherapy, and radiotherapy. However, each of these modalities has huge limitations and can expose the patient to high risks. Surgery is effective when tumors are well-defined and localized, but is by no means a cure. Surgery's largely macroscopic methods do not allow for the removal of all cancer cells, and can lead to the reappearance of tumors. Also, many tumors are inoperable as they may be too close and intertwined with vital organs. Therefore surgery is combined with chemotherapy and/or radiotherapy.

Chemotherapeutic drugs are highly toxic compounds that work by causing DNA damage and impairing mitosis, thus having the most drastic impact on rapidly dividing cells. However, this includes not only cancer cells, but also normal cells such as those found in the bone marrow and digestive tract. The side effects of these drugs can include immunosuppresion, nausea, cardiotoxicity, hepatotoxicity, and nephrotoxicity among others. Chemotherapy also ironically increases the risk of developing additional cancers.

It is therefore important to develop effective cancer treatments that can minimize the toxic side effects associated with conventional therapeutics.

Radiotherapy involves the use of ionizing radiation which ionizes the atoms that make up the DNA chain. It also works by ionizing water and other molecules to create radicals which then react with and damage DNA. While the radiation is targeted to the cancerous tissue, much of the surrounding cells are exposed to high and moderate doses of radiation. Due to this effect, many patients may develop disorders such as fibrosis, infertility, edema and even additional cancers.

In search of more effective tools to fight cancer, many novel therapies are under development. Delivery of chemotherapeutic agents using targeted nanoparticles is one of the promising approaches for increasing therapeutic effects and reducing systemic cytotoxicity (Barua & Rege, 2009; Larocque et al., 2009). The use of nanoparticles in medicine has therefore begun to explode in the last decade. These particles which are on the order of a billionth of a meter, have unique physical and chemical properties that can be used to solve clinical problems. Due to their small size, these particles are able to access places within the body that would otherwise be inaccessible (Barua & Rege, 2009; Larocque et al., 2009). Also their high surface to volume ratio allows these particles to be functionalized and specialized as necessary (Barua & Rege, 2009; Larocque et al., 2009). Therefore, their use as a drug delivery system and imaging tool is now being realized and investigated in the hopes of discovering effective therapeutics to treat cancer and a variety of other illnesses.

1.2 Nanoparticles for tumor imaging and drug delivery

1.2.1 Advantages of Nanoparticles

An important aspect in effectively treating cancer is its detection and imaging. Current imaging methodology such as CT and MRI differentiate between the morphological features of the tumor tissue and organs. Although these technologies have been improving with increasing spatial resolution, these imaging modalities have limited sensitivity and cannot provide specific and functional information about the disease.

Advances in the new field of molecular imaging focuses on the visualization of biological events in living systems (Atri, 2006). Current molecular imaging modalities such as photon emission tomography (PET), fluorescence-mediated tomography, and near-infrared fluorescence reflectance imaging (FRI) are highly sensitive (Gambhir, 2002; Kjaer, 2006). However, some of the imaging probes have limitations. For example, 18F-labeled fluorodeoxyglucose only localizes to tumors that have increased glucose uptake and metabolism, and therefore cannot detect cells that have a low glucose uptake (Mankoff et al., 2007). Cancer detection is vital for increasing patient survival. Nanoparticles as imaging contrast agents provide the possibility for the production of multifunctional nanoparticles which can provide targeted tumor imaging whilst delivering therapeutic agents. These nanoparticles offer more functionality than conventional probes as they have both greater surface areas, and more functional groups which can be linked with diagnostic and therapeutic agents.

Due to their physical dimensions, untargeted nanoparticles are able to preferentially accumulate within tumors and can provide an image of the tumor environment (passive targeting) However, one molecular strategy to improve the

specificity of cancer detection is by coupling imaging probes with ligands that can recognize and interact with target molecules that are specifically produced by cancer cells (active targeting). However, for this to be effective, the target molecule must be highly expressed in cancer cells, while being found at low or undetectable levels in normal cells. For this imaging approach to have clinical applications, the imaging probes should emit a strong enough signal to provide highly sensitive imaging while having low toxicity on normal cells. Finally, the probes should have a reasonable blood circulation retention time to allow for sufficient accumulation in the tumor mass.

Passive targeting

Nanoparticles can have many advantages even when untargeted due to their small size and the unique properties of tumors such as the enhanced permeability and retention (EPR) effect and the tumor microenvironment (Deryugina & Quigley, 2006). This enhances drug bioavailability and efficacy.

Tumor growth results in the rapid creation of blood vessels. Tumors promote angiogenesis by secreting factors such as vascular endothelial growth factor (VEGF), therefore recruiting blood vessels to provide the growing tumor with nutrients and oxygen. Without additional blood vessels, tumors cannot grow larger than 1-2mm in size (Carmeliet, 2005). However, these angiogenic blood vessels, unlike those in normal tissues, have gaps as large as 600-800nm between adjacent endothelial cells (Allen & Cullis, 2004). Along with this defective vasculature, tumors also have poor lymphatic drainage (Cuenca et al., 2006). These structural defects allow nanoparticles to extravasate through gaps in tumor vasculature and accumulate inside tumor tissues (Cuenca et al., 2006). A schematic of the EPR effect is shown below in Figure 1.

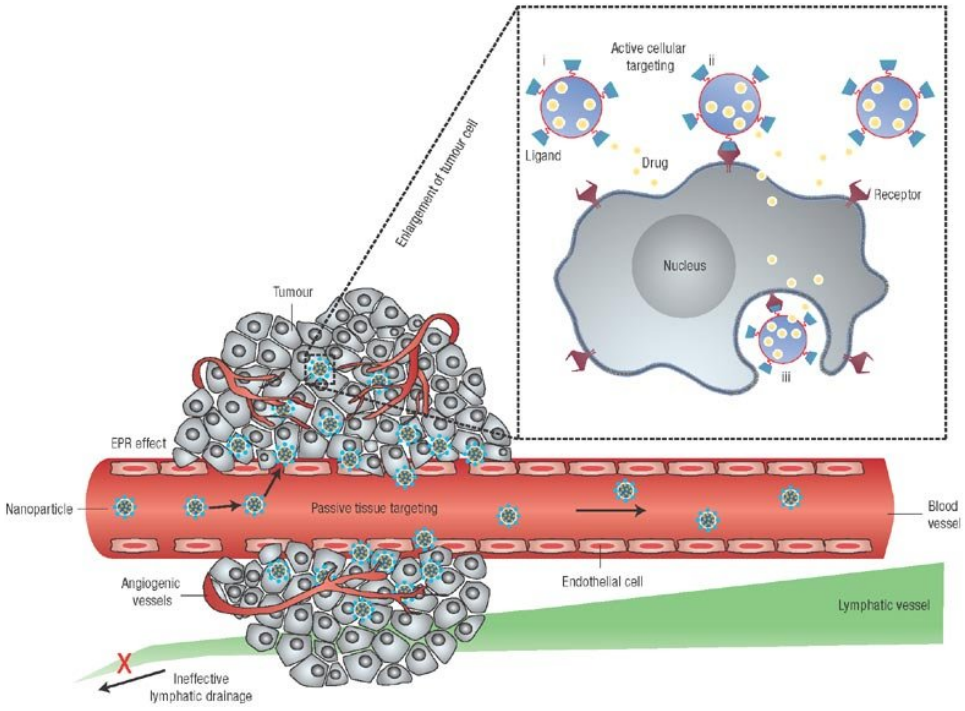

Figure 1: Schematic of EPR effect (Peer et al., 2007)

These effects can be so drastic that there can be a 10-fold or greater increase in drug accumulation simply by delivering a drug using nanoparticles rather than the free drug (Cuenca et al., 2006). The rate and amount of accumulation of the nanoparticles in tumors depends on factors such as the size, surface characteristics, and the circulation half-life of the nanoparticles as well as the degree of angiogenesis.

Hyperproliferative cancer cells and growing tumors must use glycolysis due to the hypoxic environment within tumors and/or due to the large energy requirements from rapid growth (Pelicano, Martin, Xu, & Huang, 2006). This results in an acidic environment (Pelicano et al., 2006). Additionally, cancer cells overexpress and release enzymes such as metalloproteinases (MMPs) that allow for tumor migration and metastasis (Deryugina & Quigley, 2006). This allows for prodrug therapy in which a drug

is activated when it enters the tumor microenvironment. For example, nanoparticles containing an albumin-bound form of doxorubicin (a chemotherapeutic drug) with an MMP-2–specific peptide sequence (Gly-Pro-Leu-Gly-Ile-Ala-Gly-Gln) have been created (Mansour et al., 2003). These nanoparticles release the drug in the presence of MMP-2. Liposomes embedded with MMP-2 cleavable peptides have also been synthesized (Terada, Iwai, Kawakami, Yamashita, & Hashida, 2006). In the presence of MMP-2, the peptides are cleaved, resulting in the rupture of the liposomes, and consequently the release of the drug. Also, pH sensitive molecules can be incorporated into nanoparticles. Therefore, when the nanoparticle enters the acidic tumor microenvironment, the drug will ionize and be released from the nanoparticle. Finally, pH-sensitive and thermolabile liposomes have been created that rupture in the acidic and hyperthermic environment of the tumor respectively (Kong et al., 2000; Yatvin, Kreutz, Horwitz, & Shinitzky, 1980).

Active targeting

One strategy that can be used to make nanoparticles more effective is by conjugating a targeting ligand or antibody to them. This targeting molecule binds to an antigen or receptor that is either uniquely expressed or overexpressed on the cancer cell surface. Conjugating a ligand therefore allows nanoparticles to deliver drugs to tumor tissues with greater efficiency. Different ways of functionalizing QDs are shown in Figure 2.

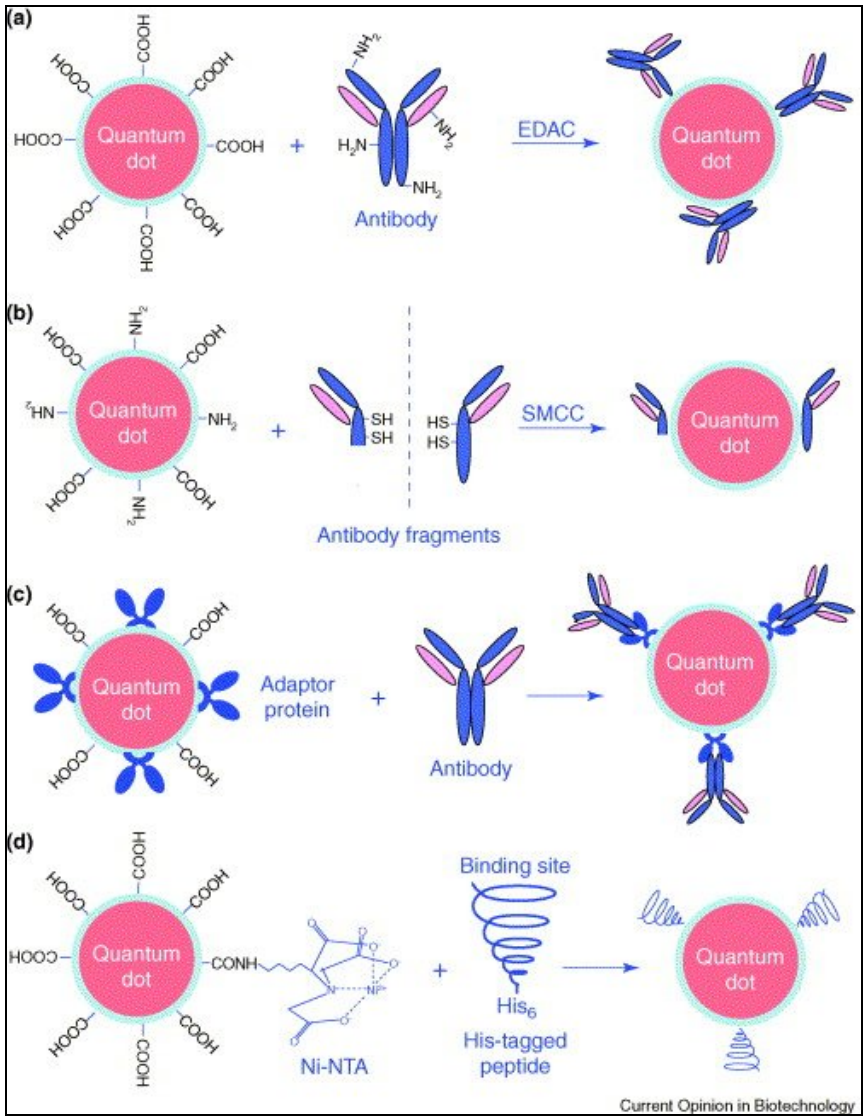

Figure 2: Various methods of functionalizing QDs (Gao et al., 2005). (a) Antibodies can be conjugated to the surface of QDs using EDAC. This reagent activates carboxylic acid groups, allowing them to readily react with the amino group to form a peptide bond. (b) Antibody fragments can be conjugated to QDs using SMCC, a reagent which activates the amino and sulfhydryl groups. (c) Adaptor proteins can be attached to the polymer coating of QDs, which can then bind to an antibody. (d) Ni-NTA microspheres can be attached to the surface of quantum dots. His-tagged proteins then bind to this complex via affinity to nickel metal.

When targeting a nanoparticle to tumor tissue using a ligand, the ligand must be selected based on an appropriate target receptor. The ideal targets are those that are abundantly and/or uniquely expressed on tumor cells but have low expression on normal

cells. Also, whether this target will result in the internalization of the nanoparticle is an important criterion in selecting a targeting ligand. If the target does not internalize the nanoparticle, the drug will only enter the cell through diffusion or other transport system after being released at the cell surface. These drugs that are released outside of the cell can disperse to the surrounding normal tissue. Therefore, it is important that the ligand bind to a target that will internalize the nanoparticle as the intracellular concentration of the drug will be much higher when the drug is released within the cytoplasm.

1.2.2 Types of Nanoparticles

Nanoparticles are small objects sized between 1 and 100 nanometers. These particles have many unique properties which can be modified according to their size (Larocque et al., 2009). They also have visible properties as they are small enough to confine their electrons to produce quantum effects (Larocque et al., 2009).

Nanoparticles can be made from a variety of materials using various manufacturing methods, allowing them to have diverse shapes, sizes, and distinct properties. Many of the nanoparticles being investigated as drug delivery systems include liposomes, iron oxide nanoparticles, and polymer-drug conjugates.

Liposomes and lipid based carriers

Liposomes are tiny vesicles that are made of phospholipids, the same molecules that make up the cell membrane. Phospholipids have a polar phosphate group as its head, and a long hydrocarbon chain as its tail. In the presence of water, the heads are attracted to it, and line up to form a surface facing the water. The long non-polar tails are repelled by the water, and form a surface away from it. As there is water on the outside and inside

the liposome, there are two layers of phospholipids, with two surfaces of heads facing the aqueous environment. This creates a phospholipid bilayer. This process is used to create bilayered vesicles known as liposomes, as shown in Figure 3.

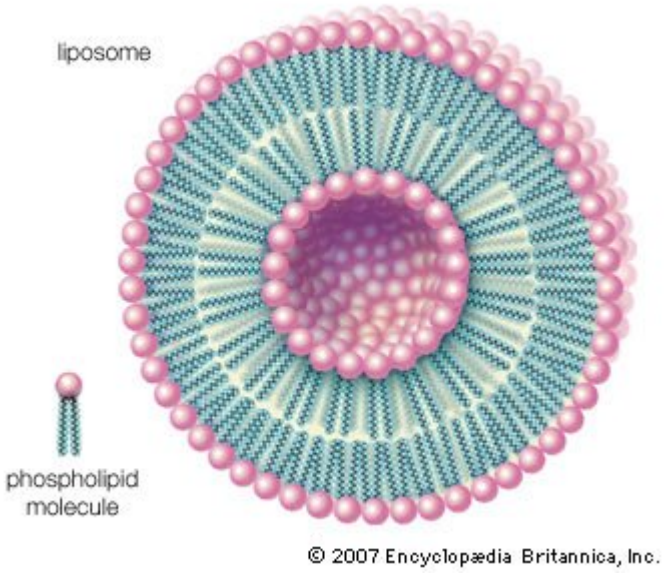

Figure 3: Structure of Liposome

Liposomes can be used for drug delivery due to their unique properties. A liposome encapsulates a region of aqueous solution inside a hydrophobic membrane (Medina, Zhu, & Kairemo, 2004). Therefore, dissolved hydrophilic drugs cannot pass through the lipid bilayer (Medina et al., 2004). These liposomes however can also carry hydrophobic drugs as they can dissolve into the membrane (Medina et al., 2004). Liposomes are then able to non-selectively deliver the molecules to the site of action by fusing with the bilayers of the cell membrane (Medina et al., 2004). However, liposomes can be targeted to tumors by conjugating antibodies or peptides to their surfaces, allowing them to enter the cell via receptor-mediated endocytosis (Medina et al., 2004). Liposomes can also deliver drugs using pH mediated release (Yatvin et al., 1980). Liposomes can be

created to contain a low or high pH, therefore charging the dissolved aqueous drugs (Yatvin et al., 1980). As the pH is neutralized within the liposomes due to the passage of protons across the membrane, the drug will also be neutralized (Yatvin et al., 1980). This neutral drug can then pass through the membrane.

As liposomes have improved pharmacokinetics and pharmacodynamics, they have been the most studied formulation of nanoparticle drug delivery. Several liposomal formulations such as Doxil (stealth liposomal doxorubicin) and DaunoXome (liposomal daunorubicin) have already been approved for the treatment of metastatic breast cancer and Kaposi's sarcoma (Fassas & Anagnostopoulos, 2005; Hofheinz, Gnad-Vogt, Beyer, & Hochhaus, 2005).

Polymeric Nanoparticles

Nanoparticles that have no surface modification are usually caught by the reticuloendothelial system, primarily when circulating through the liver and spleen (Moghimi, Hunter, & Murray, 2001). By coating the nanoparticles with hydrophilic polymers, the particles can be protected from capture by macrophages (Moghimi & Szebeni, 2003). This increased hydration also helps nanoparticles to be more soluble and less sensitive to enzymatic degradation (Moghimi & Szebeni, 2003).

This has led to the development of polymer-based drug delivery systems. These biodegradable polymers which have drugs either dissolved, encapsulated, or covalently attracted to the polymer matrix can have different structures and unique functionalities (Rawat, Singh, Saraf, & Saraf, 2006). Both natural and synthetic biodegradable polymers such as albumin and PEG respectively are being used as drug delivery systems (Rawat et al., 2006).

Several polymeric nanoparticles formulations have been approved for the treatment of cancer. Abraxane which is paclitaxel bound to albumin has been approved for the treatment of metastatic breast cancer (Gradishar, 2005). Several formulations such as Xyotax and PK1 are also in clinical trials and have shown to reduce toxicity and prolong the survival of cancer patients (Albain et al., 2006; Vasey et al., 1999).

Quantum Dots

Semiconductor quantum dots (QDs) are nanometer-sized light emitting particles with unique optical and electrical properties (Figure 4).

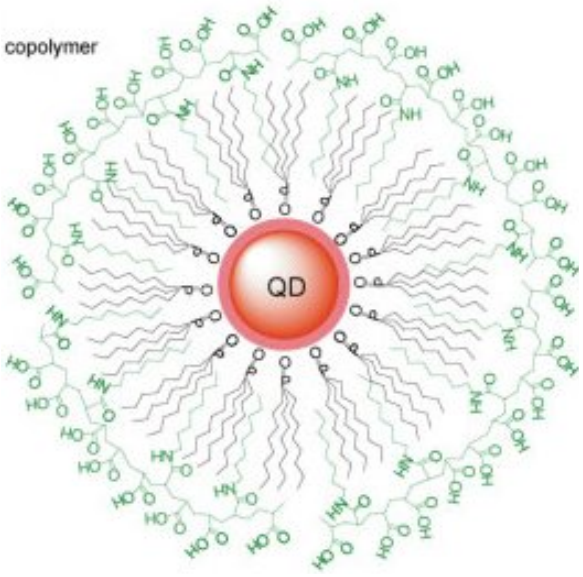

Figure 4: Structure of Quantum Dot (Chan & Nie, 1998)

Their light emission is size tunable (from 400-2000nm) and have a stable fluorescence signal with a broad absorption spectra and narrow emission profile (Chan & Nie, 1998; Larocque et al., 2009). This allows for the excitation of multiple species of QDs using a single light source without much signal cross-coupling (Chan & Nie, 1998). These properties can improve the sensitivity of molecular imaging by 1-2 orders of magnitude,

and therefore offer an alternative to traditional fluorophores (Alivisatos, Gu, & Larabell, 2005).

QDs which are hydrophilic and have a surface that is adaptable to many biological applications have been made from CdSe (cadmium selenide) (Larocque et al., 2009). However, the luminescent properties of naked CdSe nanocrystals are very sensitive to surface and solvent interactions, and therefore lead to low quantum yields. These QDs tend to be overcoated with ZnS, an inorganic material that increases luminescent yields. This class of QDs (CdSe/ZnS core/shell) offers the most promise for fluorescence-based applications.

To use QDs for imaging in biological environments, the core-shell needs to be coated with a water compatible organic material (Alivisatos et al., 2005). Thiol-containing molecules such as mercaptoacetic acid (MAA) have been used to provide QDs with water-solubility (Alivisatos et al., 2005). However, this method decreases the long-term stability of the QDs and decreases quantum yield (Alivisatos et al., 2005). Many other methods have been used to create water stable QDs, but in recent years amphiphilic di- and tri-block copolymers typically containing polyacrylic acids have been developed to encapsulate QDs (Alivisatos et al., 2005). This maintains the phospholuminescent properties of the QDs, and provides carboxylic acid functionalities which provide solubility in water and chemical functional groups for conjugation to primary amines in proteins (Alivisatos et al., 2005).

It has previously been shown that QDs can simultaneously target and image prostate tumors in animal models using bioconjugated QDs (Gao, Cui, Levenson, Chung, & Nie, 2004; Larocque et al., 2009). These QDs have an amphiphilic triblock copolymer

layer for in vivo protection, and multiple PEG molecules for improved biocompatibility and circulation (Gao et al., 2004). These QD probes are also advantageous as probes emitting at different wavelengths can be used for the imaging and tracking of multiple tumors simultaneously.

QDs producing near-infrared fluorescence (NIRF) signals have also been developed (Cai et al., 2006). As NIRF light penetrates more deeply into tissues compared with visible fluorescence, these QDs can be tracked deep inside animals unlike the several millimeter limit of visible fluorescence signals (Weissleder, 2006). These QDs are also advantageous as their emission is beyond the spectral range of the autofluorescence of blood and tissues, therefore providing imaging with a high signal-to-background ratio (Weissleder, 2006). QDs are therefore effective imaging nanoprobes for evaluating the specificity of tumor-targeting ligands in vitro and in vivo. However, since the main component of QDs is cadmium, there is concern over its potential toxicity. Its future human clinical application is unclear.

Magnetic Iron Oxide Nanoparticles

Superparamagnetic iron oxide (SPIO), or iron oxide (IO) nanoparticles, have the potential to be used clinically as they can be functionalized to become a target specific MRI contrast agent as well as drug carrier. In addition to the other properties of nanomaterials, IO nanoparticles also have a long blood-retention time and have low toxicity (Moore, Weissleder, & Bogdanov, 1997). Several forms of IO nanoparticles have already been used in clinical settings, and have been proven to be safe for human use (Hamm et al., 1994).

Recently, there has been a great interest in developing target-specific MRI contrast agents. IO nanoparticles provide this functionality as they can be conjugated with ligands targeting cellular receptors that are up-regulated in cancer cells. Also, as IO nanoparticles have low toxicity and a large surface area, their ability to deliver anticancer drugs is being actively investigated. This ability to simultaneously image and treat cancer cells has already been demonstrated by several groups (Nasongkla et al., 2006). In addition to chemotherapy drugs, IO nanoparticles can deliver small interfering ribonucleic acids (siRNAs) (Medarova, Pham, Farrar, Petkova, & Moore, 2007). These siRNA molecules can silence the expression of genes that are important to cancer cells by binding to their target transcript and leading to their degradation. IO nanoparticles are therefore multifunctional as they can serve as both a powerful contrast agent and a drug carrier.

1.3 Nanoparticle delivered chemotherapeutic agents

As previously mentioned, nanoparticle formulations of several chemotherapeutic drugs such as paclitaxel and doxorubicin have already been approved by the FDA. Doxorubicin, due to its small size compared to other chemotherapeutic agents, is ideal for use in quantum dots and iron oxide nanoparticles. It is a highly potent anthracycline antibiotic that is used in the treatment of a variety of cancers (Fornari, Randolph, Yalowich, Ritke, & Gewirtz, 1994). The planar aromatic portion of doxorubicin has been implicated in its mechanism of action (Fornari et al., 1994)(Figure 5).

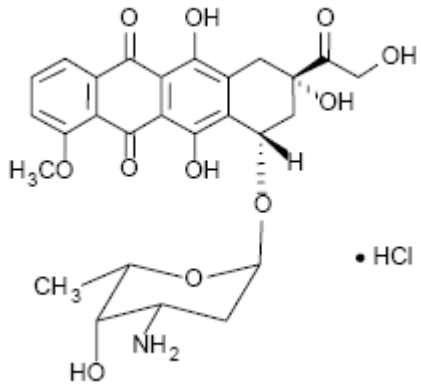

Figure 5: Structure of doxorubicin

This characteristic allows doxorubicin to intercalate between two base pairs, and sit in the minor groove of the DNA molecule (Fornari et al., 1994). By intercalating DNA, doxorubicin is able to inhibit the transcription of genes (Fornari et al., 1994). It can also inhibit topoisomerase II, a vital enzyme that unwinds DNA for transcription (Fornari et al., 1994). Doxorubicin stabilizes the topoisomerase II complex after it has nicked the DNA, therefore leaving the DNA and preventing ligation (Fornari et al., 1994).

1.4 uPAR as a target for ligand conjugated nanoparticles

For ligand conjugated nanoparticles to be highly selective for tumors, their targets should be receptors that are up-regulated in cancer cells. One receptor that is highly overexpressed in cancer cells is the urokinase plasminogen activator receptor (uPAR), a glycoprotein that contains 283 amino acids linked to the cell surface via a carboxyl-terminal glycosylphosphatidylinositol (GPI) linker (Figure 6) (Blasi & Carmeliet, 2002; Huai et al., 2006; Jo, Thomas, Wu, & Gonias, 2003).

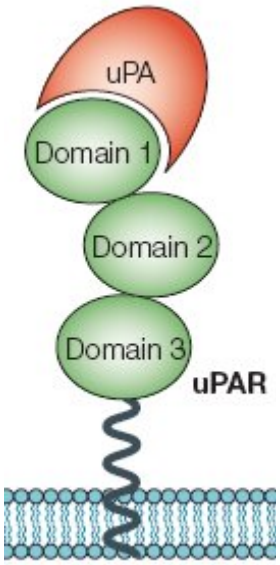

Figure 6: Structure of uPAR (Blasi & Carmeliet, 2002)

uPAR has been shown to be upregulated in more than 86% of pancreatic cancer tissues and is expressed at low levels in healthy pancreatic tissue (Yang et al., 2009). A previous study has shown that of 27 genes that are up-regulated in pancreatic cancer tissues, the level of uPAR has the highest diagnostic accuracy for the detection of pancreatic ductal carcinoma (Yang et al., 2009). Also, high levels of uPA and uPAR has been correlated with cancer progression and a poor prognosis in breast cancers and other malignancies (Jo et al., 2003). It has been quantified by flow cytometry that normal mammary epithelial cells have approximately 2,500 uPAR/cell, whereas the uPAR number in various breast cancer cells can range from 13,700 to more than 50,000 receptors per cell (Li, Wood, Yellowlees, & Donnelly, 1999). However, uPAR is upregulated not only on tumor cells, but also on most tumor endothelial cells (Sturge, Wienke, East, Jones, & Isacke, 2003). This allows for the targeting of drugs to not only tumors, but also tumor vessels. This is advantageous as it can produce an anti-

angiogenesis effect, does not rely on the receptor levels of the tumor cells, and is more unlikely to lead to drug resistance.

uPAR is a receptor for the urokinase plasminogen activator (uPA). uPA is composed of a carboxyl-terminal serine protease domain, and a modular amino-terminal fragment that contains all of the determinants required for binding to its receptor (Huai et al., 2006). This protein cleaves plasminogen, resulting in the activation of the serine protease plasmin (Huai et al., 2006). Plasmin then initiates matrix degradation, cell invasion, and angiogenesis (Huai et al., 2006). This cascade of events is initiated through the interaction of uPA with its receptor, uPAR (Huai et al., 2006). uPA binding to uPAR also activates a number of pathways such as the Ras-extracellular signal-regulated kinase (ERK) pathway that controls cancer cell migration, growth, and invasion (Figure 7) (Rao, 2003).

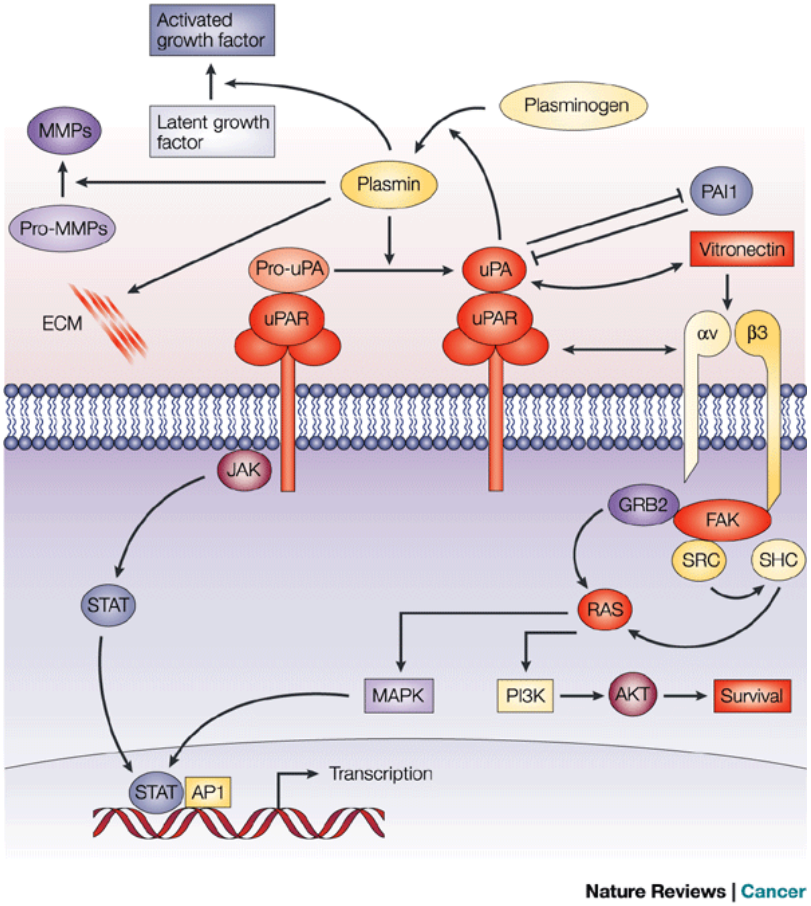

Figure 7: uPAR signaling pathways (Rao, 2003)

The binding of uPA to uPAR occurs through its modular amino terminal fragment (ATF residues 1-135 amino acids) that contains all of the residues required for binding (Figure 8)(Huai et al., 2006).

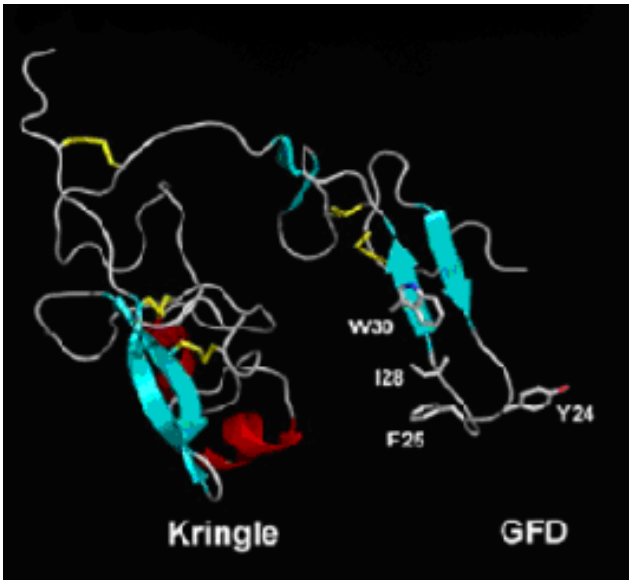

Figure 8: Structure of ATF (Huai et al., 2006)

This binding occurs with high affinity, and forms a stable complex with a K_d of 0.28 nM (Huai et al., 2006). Previous studies have showed that the ATF peptide can compete with uPA for the binding of uPAR at the surface of both tumor and endothelial cells, therefore resulting in the inhibition of tumor growth and angiogenesis (Huai et al., 2006). As its amino acid and genetic sequence is known, ATF is easily produced in large quantities through bacterial recombination. This makes ATF a viable ligand with which we can target uPAR.

1.5 Endocytosis

Once targeted nanoparticles have arrived at the cell surface, they must be internalized. There are several mechanisms by which cells can uptake exogenous material. This includes phagocytosis, macropinocytosis, receptor-mediated endocytosis, clathrin-mediated endocytosis, caveolin-mediated endocytosis, and clathrin and caveolin independent endocytosis (Barua & Rege, 2009). Internalized material is then sorted and

trafficked to different locations within the cell (Barua & Rege, 2009). However, differences in cancer cells play a significant role in the uptake, intracellular sorting, and localization of internalized material (Barua & Rege, 2009). As nanoparticles hold great promise in the detection and treatment of disease, an understanding of the fate of targeted and untargeted nanoparticles in cancer cells can facilitate the design and engineering of nanoparticles that can effectively target specific intracellular locations. Receptor expression profiles of cancer cells influence the intracellular trafficking of targeted nanoparticles. It has been shown that untargeted QDs are internalized from clathrin coated pits (Barua & Rege, 2009). The nanoparticles are then trafficked in vesicles along microtubules to the sorting endosomal complex (Barua & Rege, 2009). Following this stage, the nanoparticles can be sent to different fates depending on the cell phenotype. They can either be trafficked in vesicles along the lysosomal degradation pathway, retrograde transport pathway, or be transported to the perinuclear recycling compartment (Barua & Rege, 2009).

Targeted nanoparticles on the other hand enter cells mainly via receptor-mediated endocytosis, and therefore follow a more defined pathway within the cell (Figure 9).

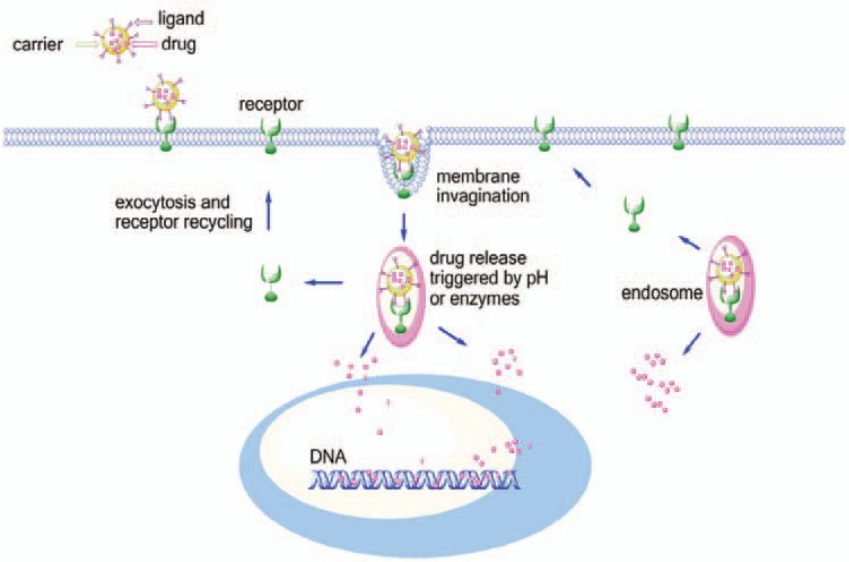

Figure 9: Diagram of targeted nanoparticle endocytosis and drug release, followed by receptor recycling (Barua & Rege, 2009)

This path is determined by the receptor to which it is targeted. As the nanoparticles in this study are targeted to the uPA receptor, it is important to determine the mechanism of endocytosis as this can affect the ability of these nanoparticles to enter cells.

As previously mentioned, uPAR is a glycosylphosphatidylinositol-anchored protein (Jo et al., 2003). Because uPAR is GPI-linked, adaptor proteins are necessary to transmit signaling responses (Jo et al., 2003). Therefore, a number of proteins have been implicated in uPAR-mediated signaling such as integrins, the epidermal growth factor receptor, FPR-like receptor-1/lipoxin A4 receptor, and caveolin (Jo et al., 2003). It has previously been shown that GPI-linked proteins cluster in plasma membrane conformations called caveolae (Stahl & Mueller, 1995; Wei, Yang, Liu, Wilkins, & Chapman, 1999). Caveolae are membrane invaginations on the cell surface that have a characteristic coat containing a protein called caveolin (Stahl & Mueller, 1995).

It has also been proposed that caveolin functions as a transmembrane adaptor protein that couples GPI-anchored proteins with cytoplasmic signaling molecules (Stahl

& Mueller, 1995; Wei et al., 1999). However, the mechanism by which GPI-linked proteins can activate cellular signaling pathways is currently unknown. The close spatial association between uPAR and caveolin suggests that caveolin could be involved in signal transduction and endocytosis mediated by uPAR (Stahl & Mueller, 1995).

As the structural integrity of caveolae depends on cholesterol, cholesterol binding drugs interfere with the structure of caveolae (Hailstones, Sleer, Parton, & Stanley, 1998; Stahl & Mueller, 1995). This has been shown to reduce the rate of surface plasmin generation, indicating that the clustering of uPAR in caveolae enhances surface plasminogen activation (Stahl & Mueller, 1995). This demonstrates that uPAR enhances uPA's catalytic activity partly by being localized in caveolae. Caveolae is therefore a cell membrane specialization that is involved in the regulation of cell activation and pericellular proteolysis.

However, whether uPAR enters the cell via a caveolin-mediated endocytotic process is unknown. It is known that uPAR is removed from the cell surface via clathrin coated pits and then recycled back (Stahl & Mueller, 1995). However, clathrin-independent internalization routes for uPAR have been reported in MDCK cells, indicating that uPAR might also be internalized by other mechanisms (Stahl & Mueller, 1995).

Caveolin-1 is a 22 kDa protein that is the main component of caveolae in plasma membranes (Senetta et al., 2009). Therefore, it is probable that caveolin-1 plays a role in uPAR internalization and can affect the entry of ATF-conjugated nanoparticles. If it is seen that caveonlin-1 plays an important role in uPAR-mediated endocytosis, it may be possible to determine the exact route of uPAR-targeted nanoparticles within the cell,

providing the possibility to create additional functionalities that will allow for the intracellular targeting of nanoparticles. It may also allow caveolin-1 to be used as a biomarker to predict the efficacy of uPAR-targeted quantum dots on tumors and their vasculature. As caveolin-1 and uPAR are up-regulated in the endothelial cells of most tumor vessels, it is possible that uPAR-targeted nanoparticles are able to accumulate within tumors via caveolae-mediated transcytosis. In this mechanism, uPAR-targeted nanoparticles will be absorbed in the vasculature, transported across the interior of the cell, and be ejected from the other side. This will not only effectively pump the nanoparticles into the tumor environment, but can also allow nanoparticles to accumulate within the endothelia. This will result in an anti-angiogenic effect. However, some tumors downregulate caveolin-1, potentially affecting the efficacy of uPAR-targeted nanoparticles. Also normal endothelia express low levels of caveolin-1. If this protein does affect uPAR-mediated endocytosis, this may prevent both the transport of uPAR-targeted nanoparticles into normal tissues, and their accumulation within the endothelial cells. An illustration of this proposed method of caveolin-1 mediated accumulation of uPAR-targeted nanoparticles is shown in Figure 10.

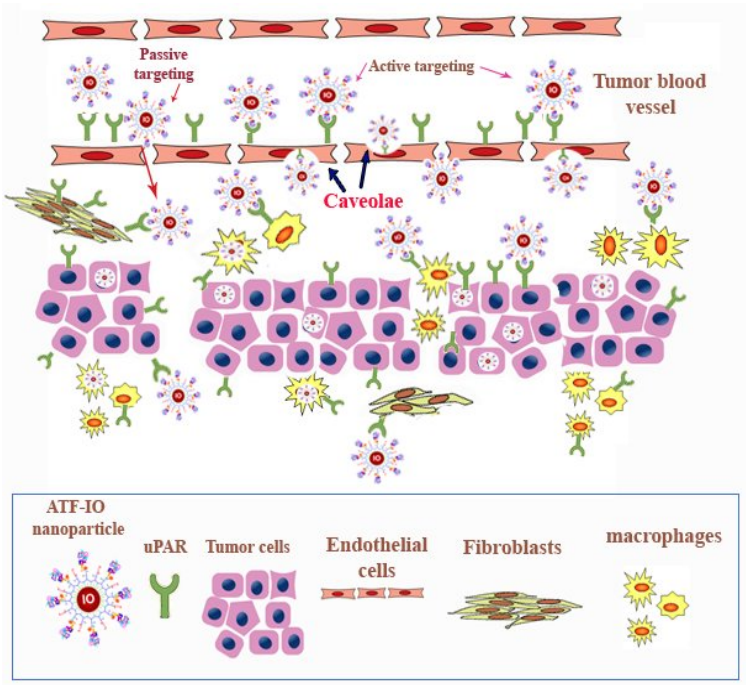

Figure 10: Schematic illustration of the proposed mechanisms for the accumulation of uPAR-targeted nanoparticles in the tumor mass (Yang et al., 2009)

1.6 Objectives

To goal of this thesis is to investigate and determine how effective uPAR-targeted quantum dots are in killing cells compared to the free chemotherapy drug. This will be determined using biomass assays. Another goal is to qualitatively determine how much more effective targeted nanoparticles are in entering cells than non-targeted nanoparticles. This will be quantified using spectroscopy, and visualized using fluorescence microscopy. A hypothesis as to how this internalization occurs is that uPAR-ligand nanoparticle complexes interact with caveolin-1 to facilitate their endocytosis. Therefore, it will be determined if caveolin-1 plays an important role in uPAR-mediated endocytosis. It will also be determined whether caveolin-1 plays a role in the non-selective endocytosis of untargeted quantum dots. These effects will be determined via spectroscopy, fluorescence microscopy, and biomass assays.

The use of quantum dots in this thesis is a model system for the determination of mechanism of drug delivery using uPAR-targeted nanoparticles since the dynamic changes in the location of quantum dots can be monitored easily. However, current generation quantum dots are not appropriate for in vivo delivery of therapeutics in humans since the potential toxicity of quantum dot treatment is currently unknown.

MATERIALS AND METHODS

2.1 Materials

Quantum dots (cadmium selenide/zinc sulfide core-shell nanocrystals) with emission maxima at 620nm and modified with an amphiphilic copolymer with carboxylic acid surface groups were obtained from OceanNanotech, LLC.

2.2 Cell Cultures

MS1 murine endothelial cell line was provided by Dr. Jack Arbiser at Emory University. These cells were grown in Dulbecco's modified Eagle's medium (DMEM) containing 4.5 g/L glucose and supplemented with 10% FBS and 1% 100X penicillin streptomycin solution. MAE murine aortic endothelial (wild-type and caveolin-1 knockout) cells were provided by Dr. Hanjoong Jo at Emory University. These cells were grown in Dulbecco's modified Eagle's medium (DMEM) containing 1g/L glucose and supplemented with 10% FBS, 1% non-essential amino acid solution (100X), 1% 100X penicillin streptomycin solution, and 100μg/mL endothelial cell growth supplement from bovine neural tissue.

2.3 Production of Mouse ATF Peptides

The DNA sequence encoding the first 135 amino acids (+ C-terminal His6 tag that was added to the sequence to facilitate purification by Ni^{2+}-NTA agarose beads, Qiagen) of the Amino Terminal Fragment (ATF) of the mouse protein that binds to urokinase plasminogen activator receptor (uPAR) was cloned pET101/D-TOPO expression vector (Invitrogen). Recombinant ATF peptides were expressed in Escherichia

coli BL21 (Invitrogen) and purified from bacterial extracts under native conditions using an Ni^{2+} NTA-agarose column (Qiagen).

2.4 Preparation of QD-Dox and QD-mA-Dox

Doxorubicin was added to the QD nanoparticles (unconjugated and conjugated) in a 1:500 ratio (QD:Dox). After four hours at room temperature, the excess doxorubicin was removed by spinning the solutions through a Nanosep 30k column.

2.5 Preparation of uPAR-targeted QD-ATF

QD nanoparticles were coated with amphiphilic polymers. The quantum dots were added to a PBS solution at pH 5.5. The carboxylic acid coat of the QDs was activated using 1um of a 8mM solution of *N*-Hydroxysuccinimide (NHS), and 1um of a 5mM solution of 1-ethyl-3-(3-dimethylaminopropyl) carbodiimide hydrochloride (EDAC). Excess NHS and EDAC were removed by spinning the solution through a Nanosep 30k column. PBS at pH 8.8 was then added to the solution mixture. Mouse ATF (mA) peptides were added to this solution mixture in a 1:10 ratio (QD: peptide).

2.6 Cell Treatment

MS1 and MAEC cells were treated with varying QD concentrations (1nM, 3nM, and 5nM) or varying doxorubicin equivalents (500nM, 1.5uM, 2.5uM respectively) in OptiMEM. The QDs and doxorubicin were removed, and cells washed after 2 hours of incubation. The cells were then fixed at various time points using a 4% formaldehyde solution.

2.7 Crystal Violet Biomass Assay

Cells were washed with PBS, followed by the addition of 50uL of the crystal violet solution. The cells were incubated at room temperature for 10 minutes. Wells were then washed in tap water by immersing plates in a beaker of water. The wells were then air dried, followed by the addition of 100uL of a 1% SDS solution. The absorbance of each well was then read at 570nm.

2.8 Spectroscopy

Cells in 96-well plates were placed in a spectrophotometer to quantify the amount of quantum dots and doxorubicin in each well. Doxorubicin was excited at 480nm and emission recorded at 560nm. The quantum dots were excited at 410nm and emission recorded at 620nm. The doxorubicin contribution to emission at 620nm was subtracted from the value of the quantum dot fluorescence, and vice versa.

2.9 Cell Visualization

After cell fixation, the nucleus was stained with the Hoechst 33342 strain. An inverted fluorescence microscope (Olympus IX51) was then used to visualize the cells. The Metamorph imaging software was used process and merge images.

RESULTS

3.1 Internalization of unconjugated and uPAR-targeted quantum dots

Conjugated and unconjugated quantum dots were incubated with MS1 cells in vitro. As the cells were incubated with the quantum dots for 2 hours, there is an increase in the amount of quantum dots in the cells between the 1 hour and 2 hour time point though this is more noticeable in the QD-mA treated cells (Figures 11&12). As expected, there is no increase in overall quantum dot fluorescence between the 2 hour and 4 hour groups (Figures 12&13). However, it is noticeable that the quantum dots are more localized around the nuclei in the 4 hour group compared with the other time points (Figures 11-13). The uPAR-targeted groups had a remarkably higher overall fluorescence when compared to the untargeted groups (Figures 11-13). Conjugated QD fluorescence is focused around the nuclei even at the 1 hour time point, whereas unconjugated QDs remain diffused throughout the cytoplasm for a longer period of time, as it is only in the 4 hour group that the quantum dots begin to aggregate around the nucleus.

(A)

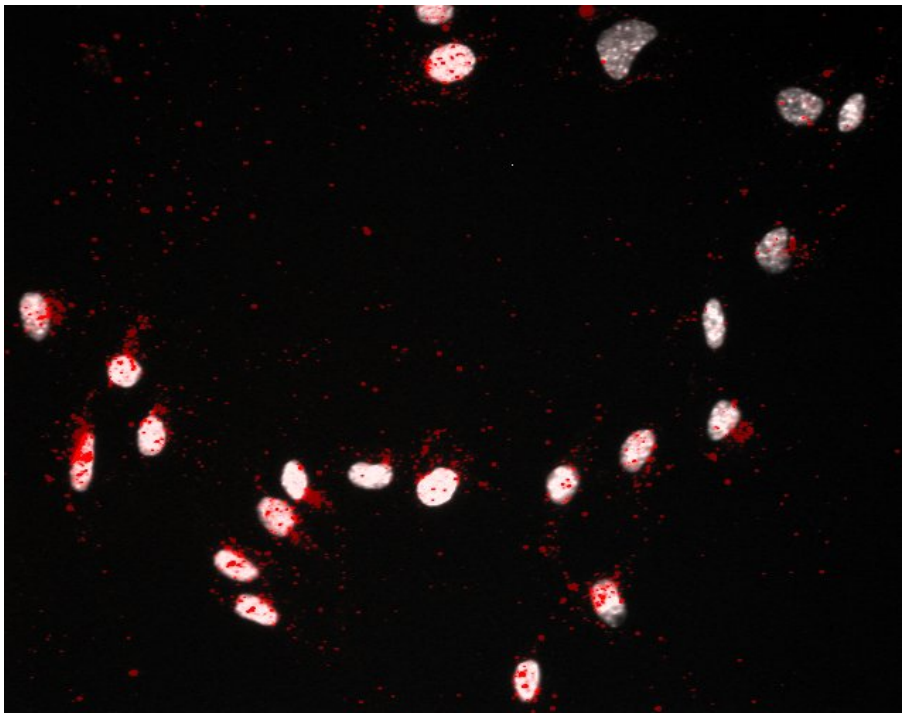

(B)

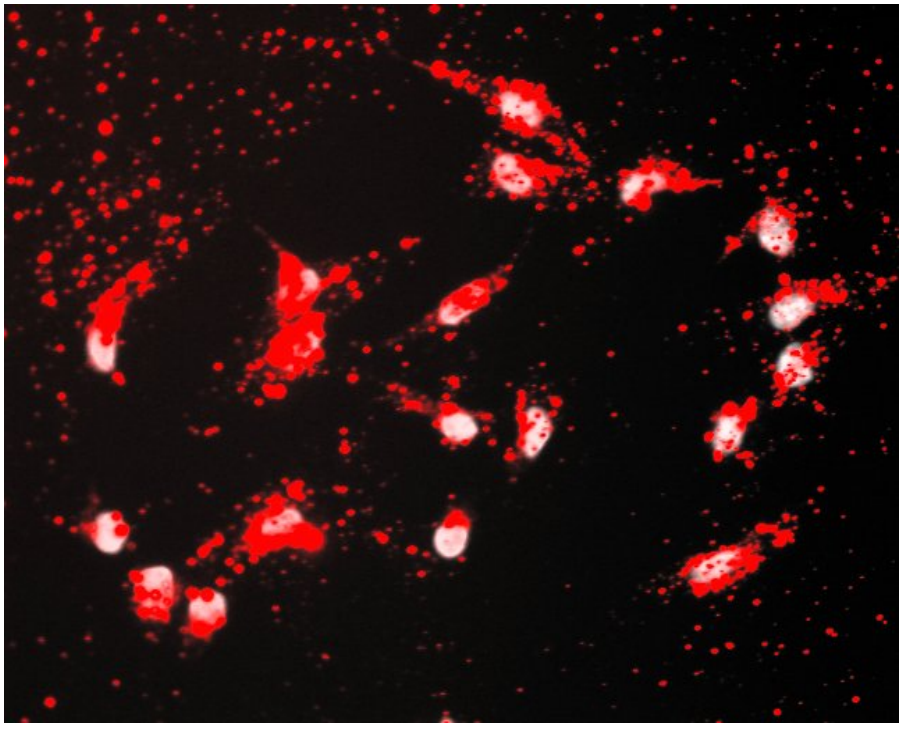

Figure 11: Fluorescence microscopy images of MS1 cells 1 hour after beginning treatment. Images of cell nuclei (white) were overlapped with images of the quantum dots (red). (A) MS1 cells treated with untargeted quantum dots. (B) MS1 cells treated with uPAR-targeted quantum dots.

(A)

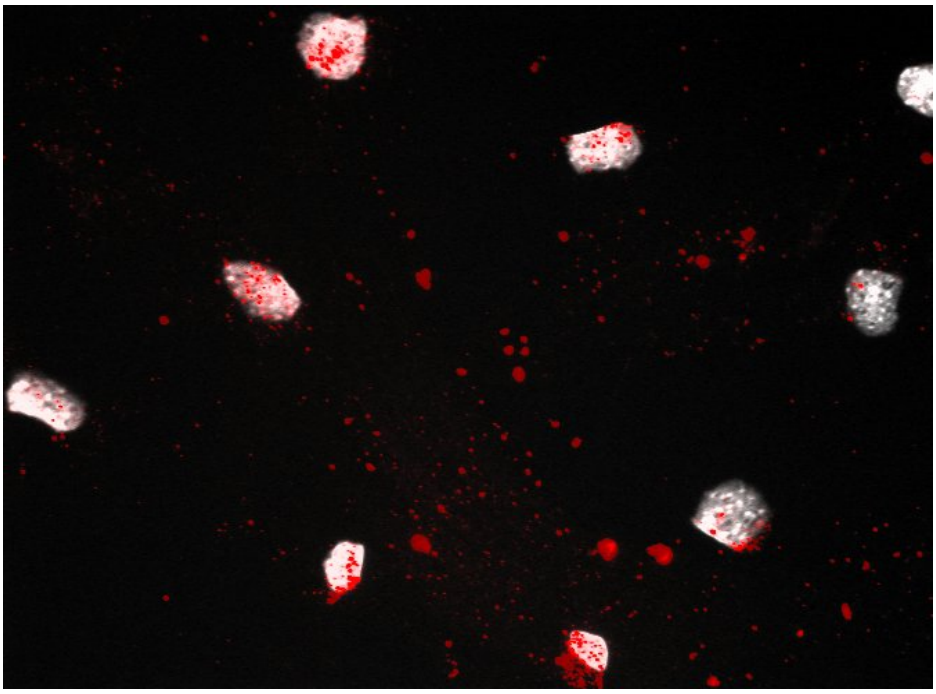

(B)

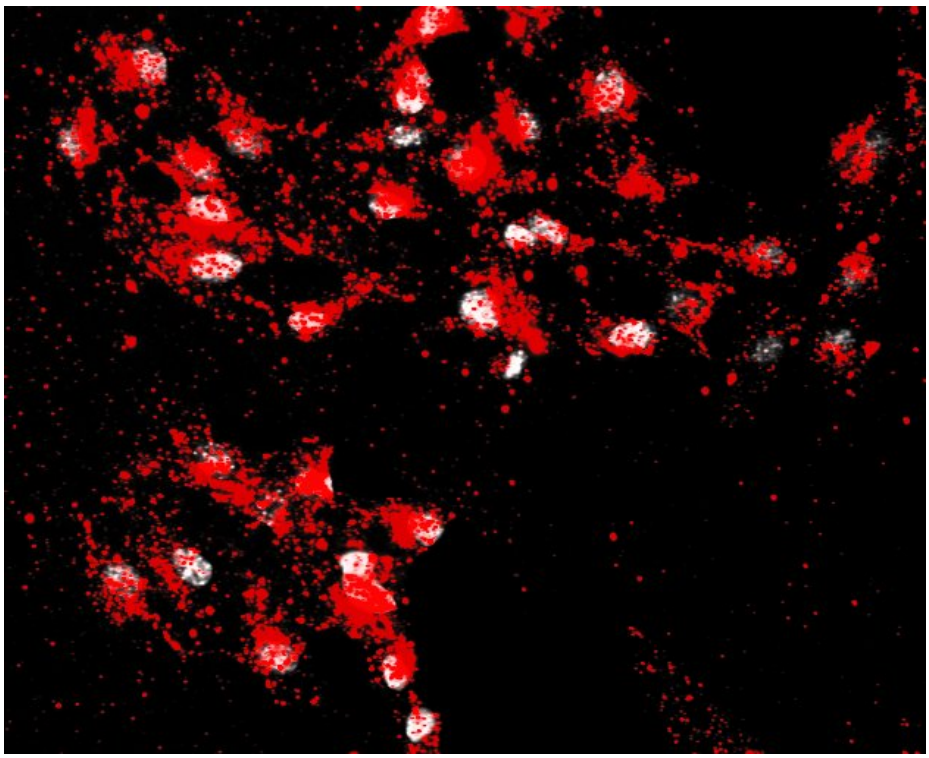

Figure 12: Fluorescence microscopy images of MS1 cells 2 hours after beginning treatment. Images of cell nuclei (white) were overlapped with images of the quantum dots (red). (A) MS1 cells treated with untargeted quantum dots. (B) MS1 cells treated with uPAR-targeted quantum dots.

(A)

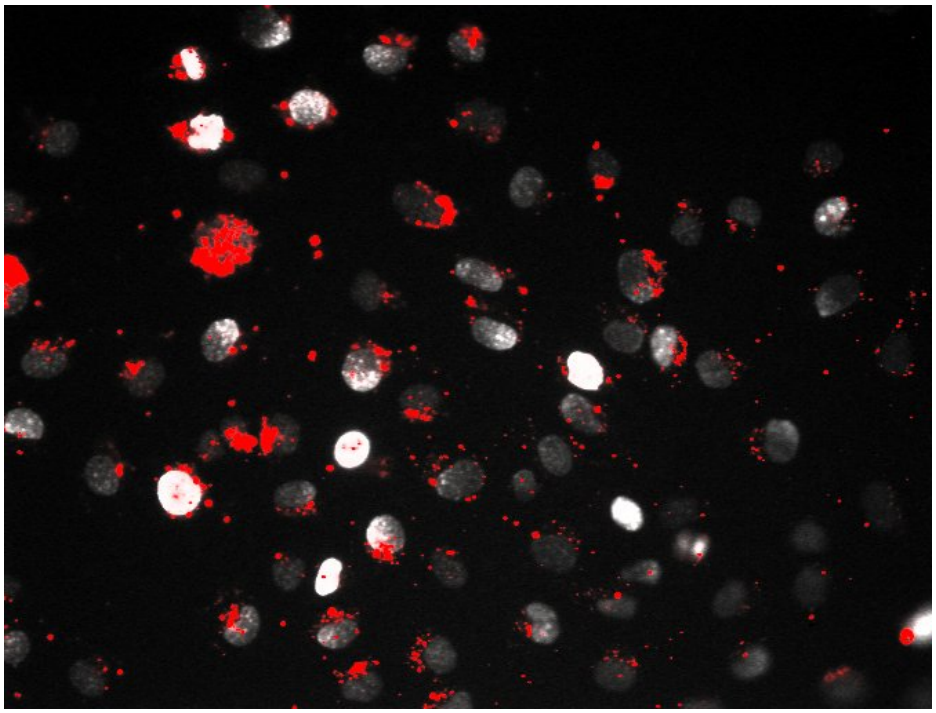

(B)

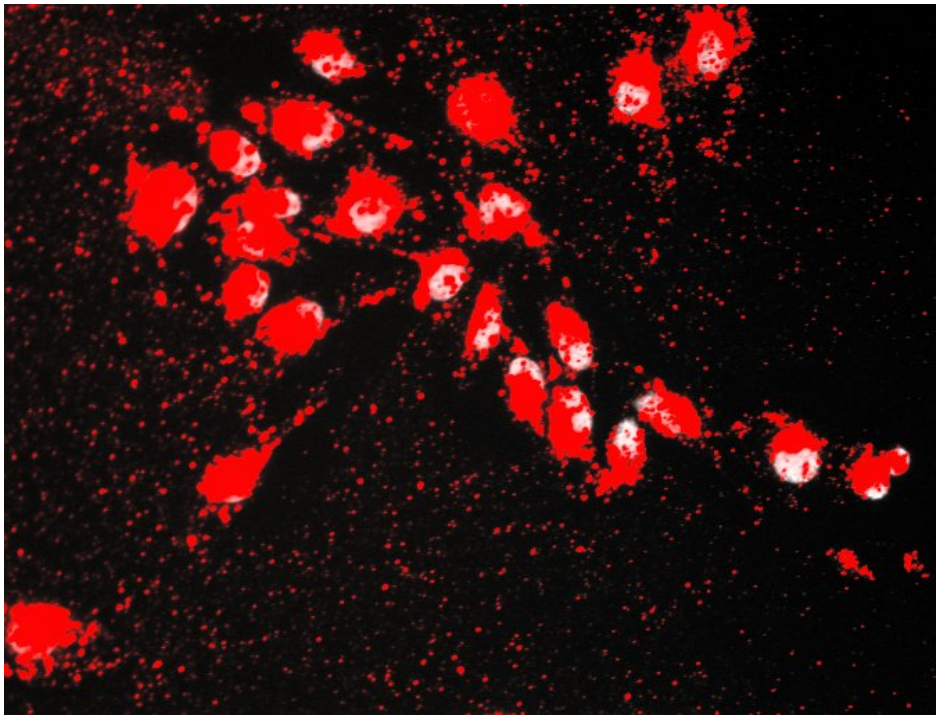

Figure 13: Fluorescence microscopy images of MS1 cells 4 hours after beginning treatment. Images of cell nuclei (white) were overlapped with images of the quantum dots (red). (A) MS1 cells treated with untargeted quantum dots. (B) MS1 cells treated with uPAR-targeted quantum dots.

3.2 Efficacy of uPAR-targeted quantum dots

The number of cells remaining after treatment was compared to number at the start of treatment (control). Although the cells were treated with various amounts of quantum dots and free doxorubicin, there were comparable effects on cell numbers. After being treated with free QDs, the cells were able to grow, although at a reduced rate (Figure 14). However, after the 48 hour time period, the number of cells after treatment was comparable in cell numbers to the control, with the exception of the 5nM group in which the QDs resulted in a decrease in cell number (Figure 14). Also at all concentrations of free QDs, there is a peak in the number of cells at ~24 hours, followed by a decrease (Figure 14). A similar effect is seen with the QD-mA (targeted QDs without doxorubicin) group (Figure 14). The QD-dox group resulted in approximately a 10% decrease in cell numbers at all concentrations (Figure 14). The free doxorubicin group also followed a similar pattern, although it was slightly more effective than QD-dox in resulting in cell death (Figure 14). The uPAR-targeted QDs on the other hand were able to significantly reduce cell numbers, especially at the 3 and 5nM concentrations (Figure 14). This effect correlates with the accumulation of uPAR-targeted QDs within cells as seen in Figures 11-13. All of the compounds possessed strong dose-dependant cytotoxic activity.

(A)

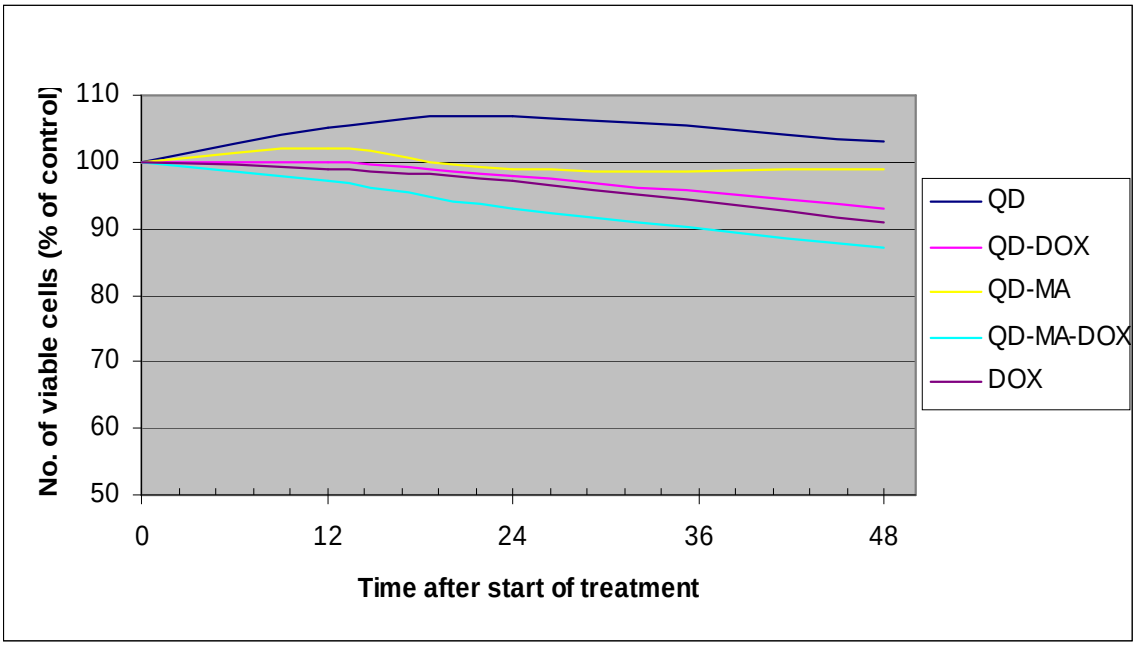
No. of viable cells (% of control)
110
100
90
80
70
60
50
0
12
24
36
48
Time after start of treatment
QD
QD-DOX
QD-MA
QD-MA-DOX
DOX

(B)

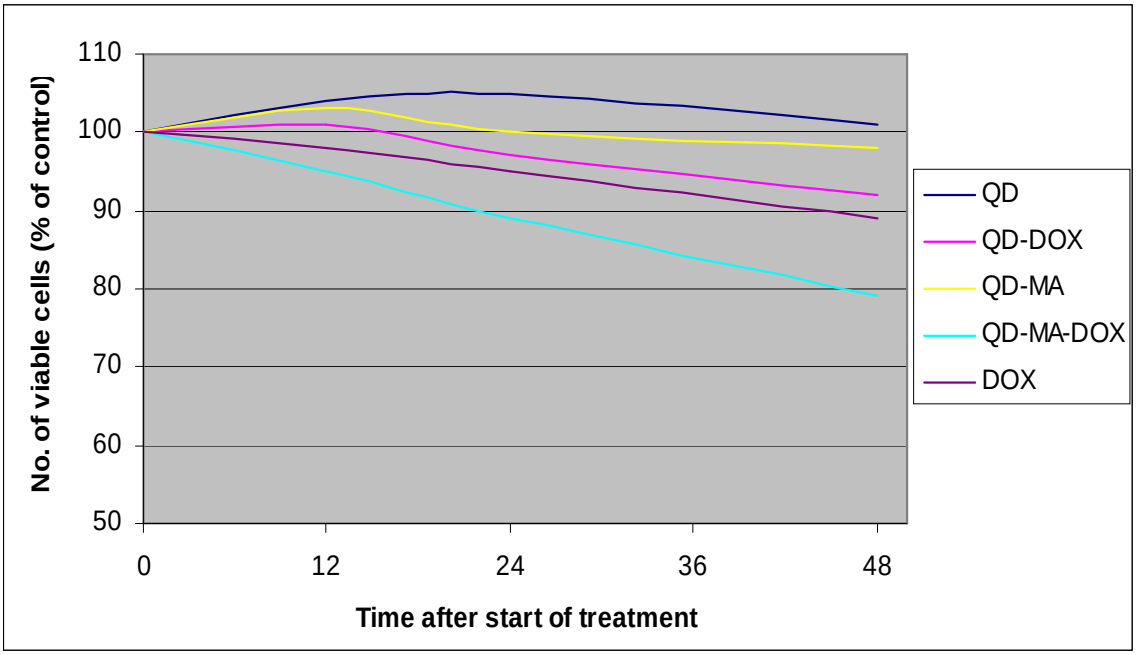
No. of viable cells (% of control)
110
100
90
80
70
60
50
0
12
24
36
48
Time after start of treatment
QD
QD-DOX
QD-MA
QD-MA-DOX
DOX

(C)

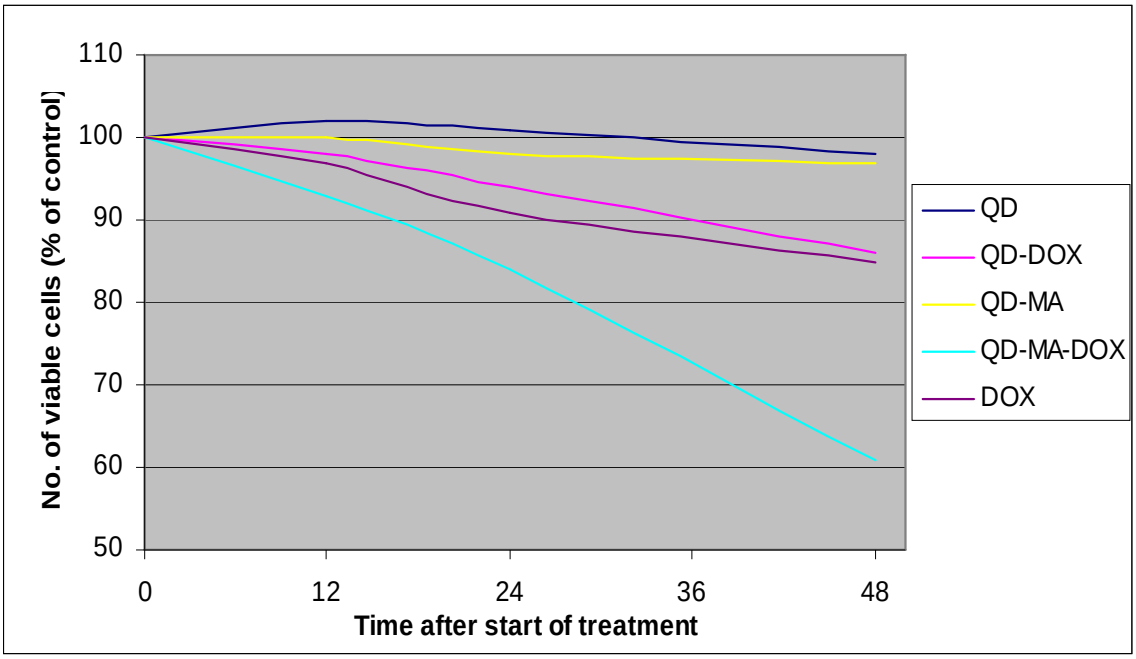

Figure 14: MS1 cells were treated with different combinations of quantum dots and free doxorubicin. The percent of cells remaining after 12, 24, and 48 hours post- treatment is compared to the number of cells at the start of treatment. The percent of cells remaining after treatment with (A) 1nM concentration of quantum dots (500nM free doxorubicin equivalent), (B) 3nM concentration of quantum dots (1.5uM free doxorubicin equivalent), (C) 5nM concentration of quantum dots (2.5uM free doxorubicin equivalent).

3.3 Effect of Caveolin-1 knockout on the internalization of unconjugated and uPAR-targeted quantum dots

Targeted and untargeted QDs were incubated with MAE (wild-type and caveolin-1 knockout) cells in vitro. Again, as the cells were incubated with the QDs for 2 hours, there is an increase in the amount of quantum dots between the 1 and 2 hour time points (Figures 15-17). It can bee seen that there is slightly more unconjugated quantum dots in the wild-type cells than in the caveolin-1 knockout cells at all time points (Figures 15-17). This is more noticeable at 1 hour, and more difficult to distinguish at the later time points due to background fluorescence (a result of quantum dots attached to the plate).

(A)

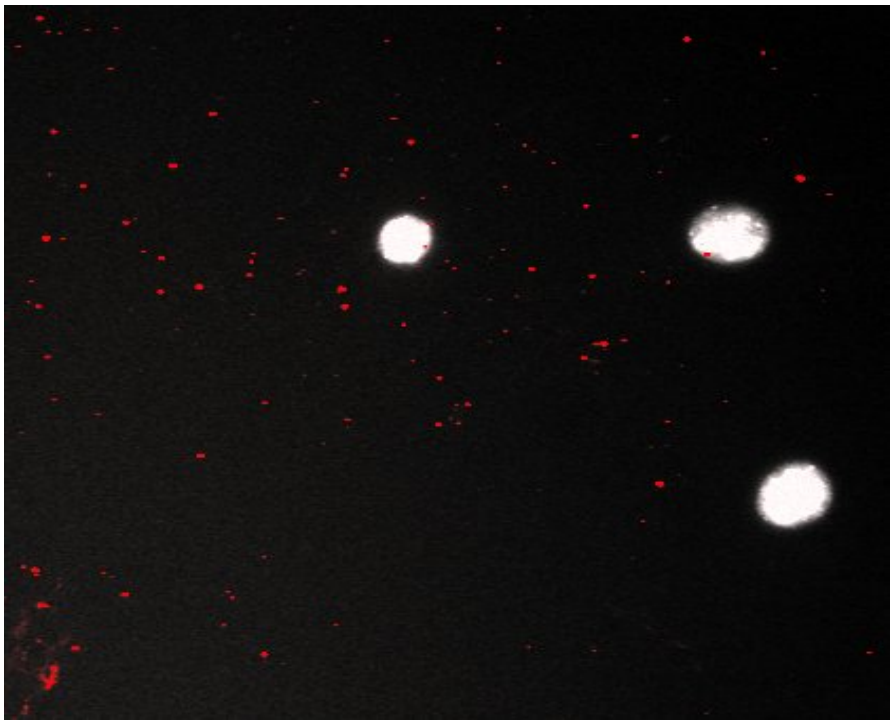

(B)

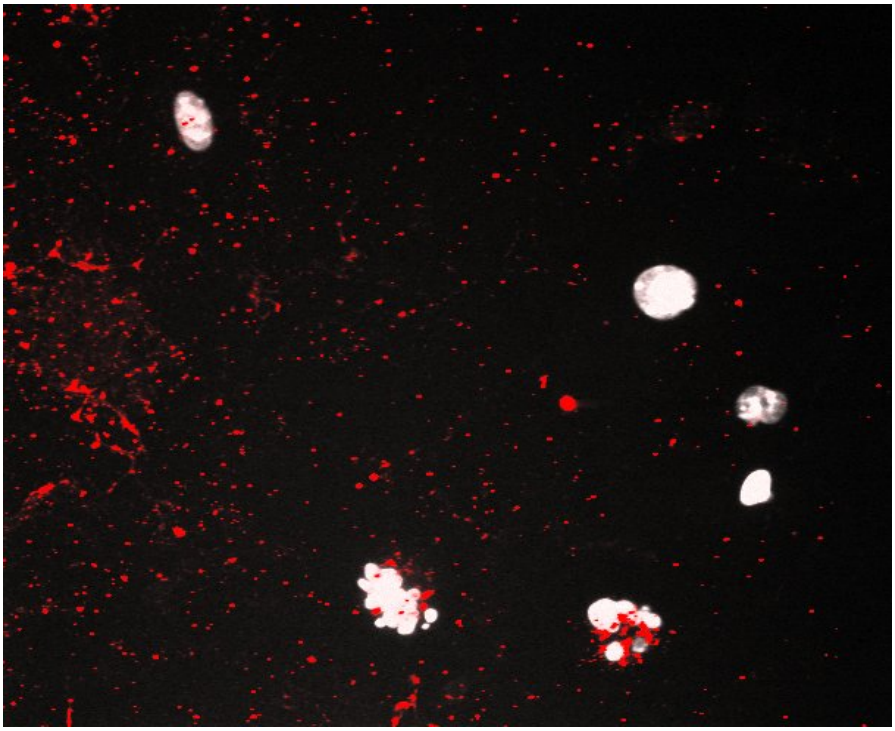

Figure 15: Fluorescence microscopy images of MAE cells 1 hour after beginning treatment. Images of cell nuclei (white) were overlapped with images of the quantum dots (red). (A) MAE caveolin-1 knockout cells (B) MAE wild-type cells treated with untargeted quantum dots.

(A)

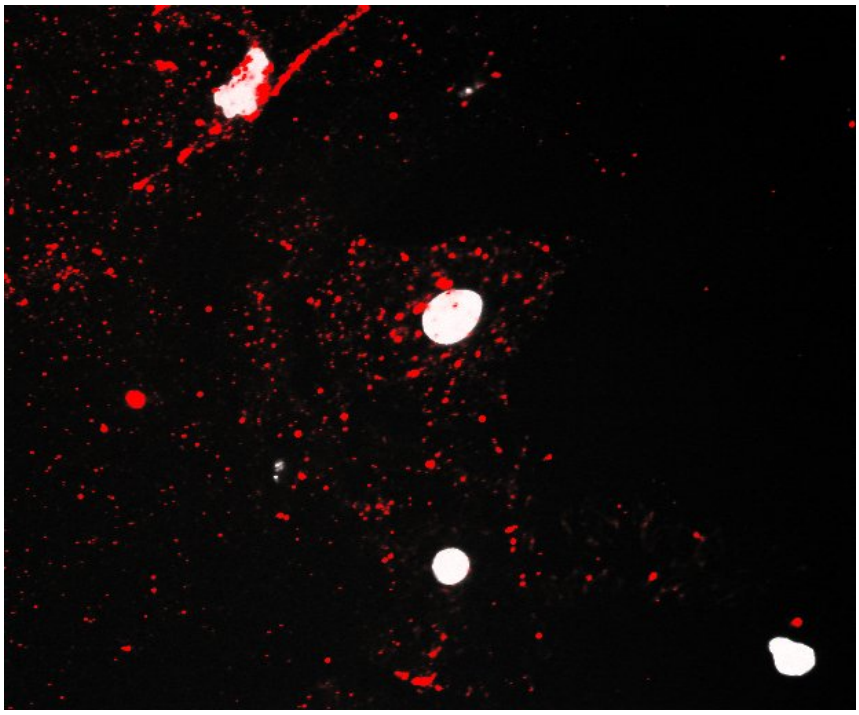

(B)

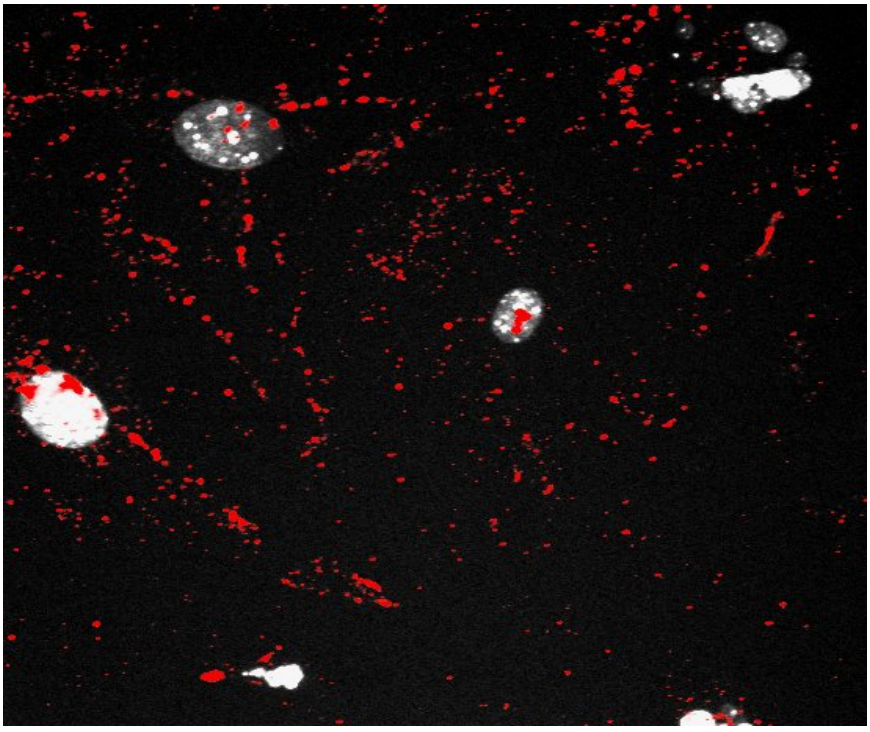

Figure 16: Fluorescence microscopy images of MAE cells 2 hours after beginning treatment. Images of cell nuclei (white) were overlapped with images of the quantum dots (red). (A) MAE caveolin-1 knockout cells (B) MAE wild-type cells treated with untargeted quantum dots.

(A)

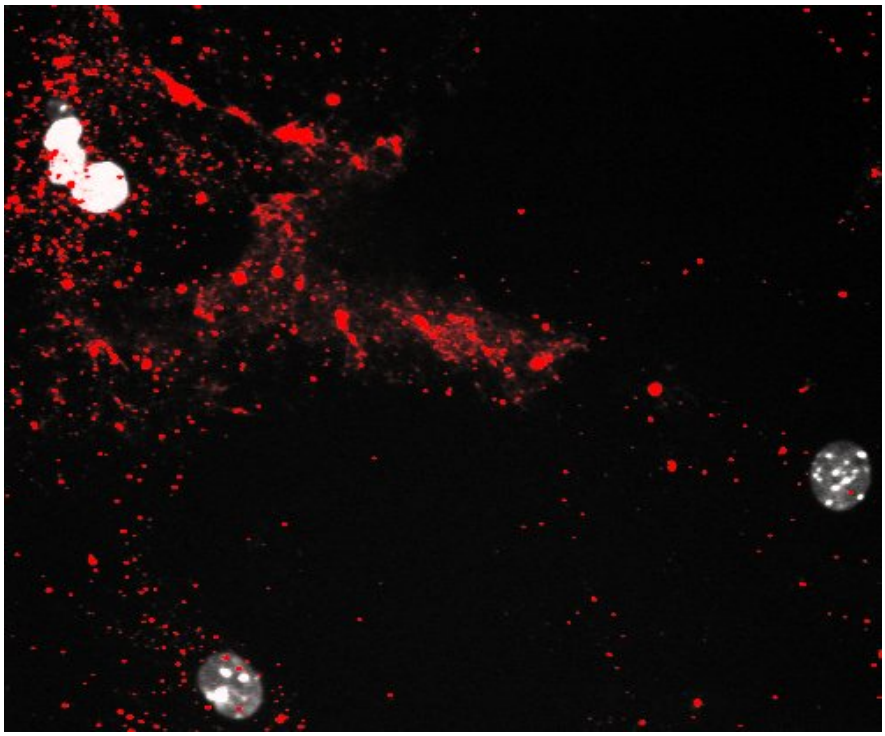

(B)

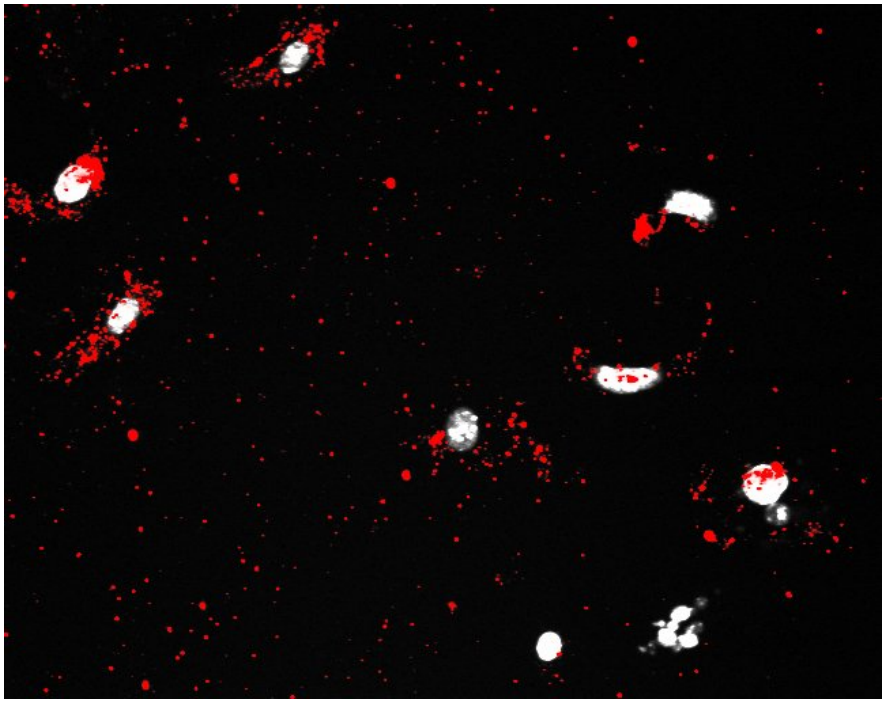

Figure 17: Fluorescence microscopy images of MAE cells 4 hours after beginning treatment. Images of cell nuclei (white) were overlapped with images of the quantum dots (red). (A) MAE caveolin-1 knockout cells (B) MAE wild-type cells treated with untargeted quantum dots.

The uPAR-targeted groups had a higher overall fluorescence, and more nuclear localization when compared to the untargeted groups (Figures 18-20). Wild-type MAE cells also contained more targeted quantum dots in their cell bodies when compared to caveolin-1 knockout cells (Figures 18-20). This is difficult to see in Figure 20A due to background fluorescence. Wild-type MAE cells (Figure 20B) had most of its quantum dots located perinuclearly, indicating that the quantum dots are in fact within the cell bodies. However, most of the quantum dots seen in Figure 20A have attached to the well as there is no visible accumulation within the cell bodies. It can also be seen that quantum dots more readily localized to the nucleus in wild-type cells (Figures 18-20).

(A)

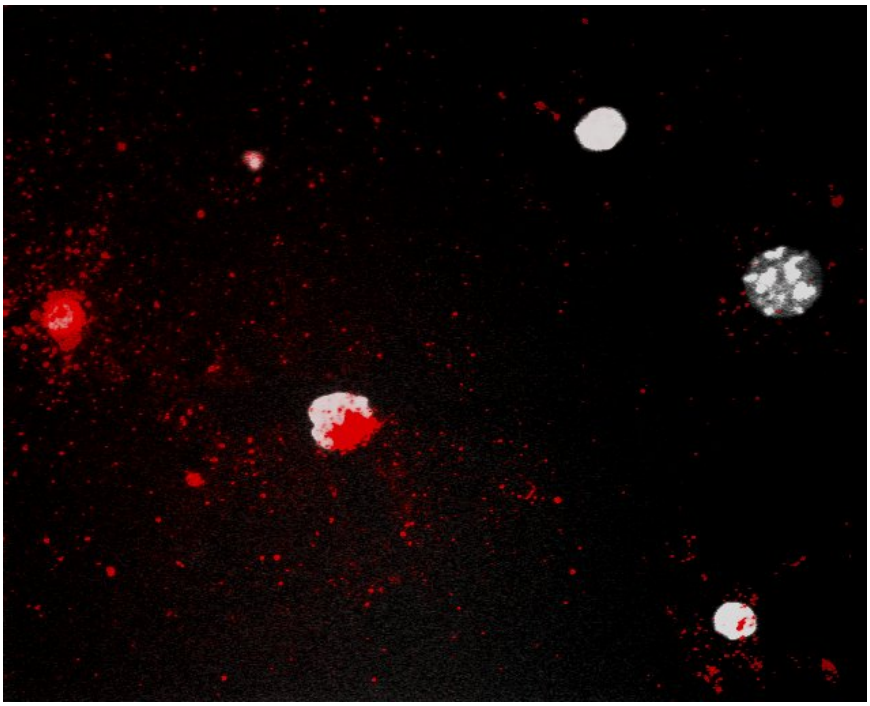

(B)

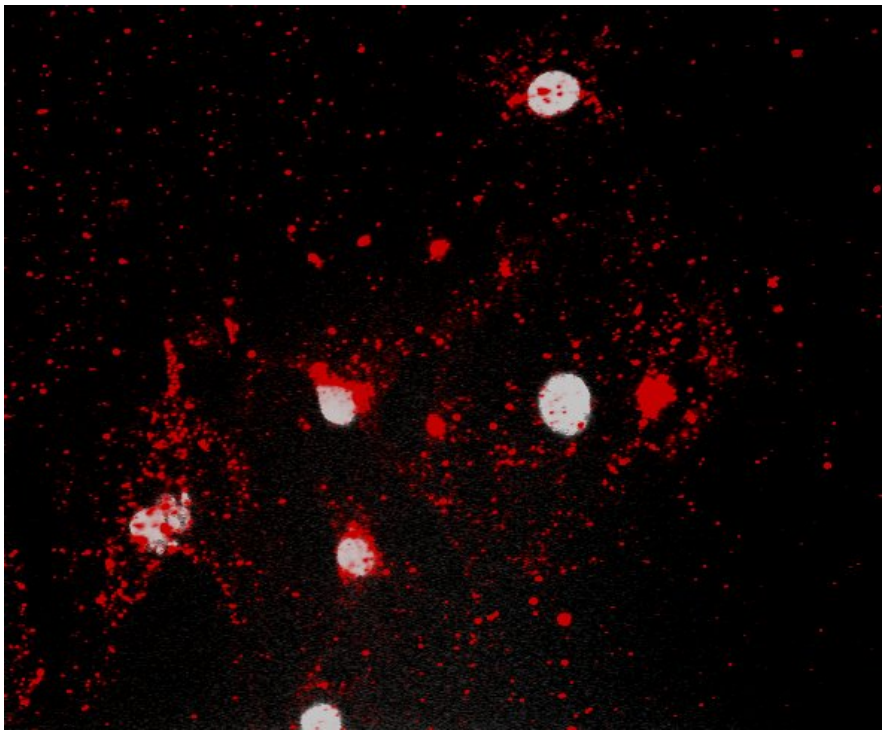

Figure 18: Fluorescence microscopy images of MAE cells 1 hour after beginning treatment. Images of cell nuclei (white) were overlapped with images of the quantum dots (red). (A) MAE caveolin-1 knockout cells (B) MAE wild-type cells treated with targeted quantum dots.

(A)

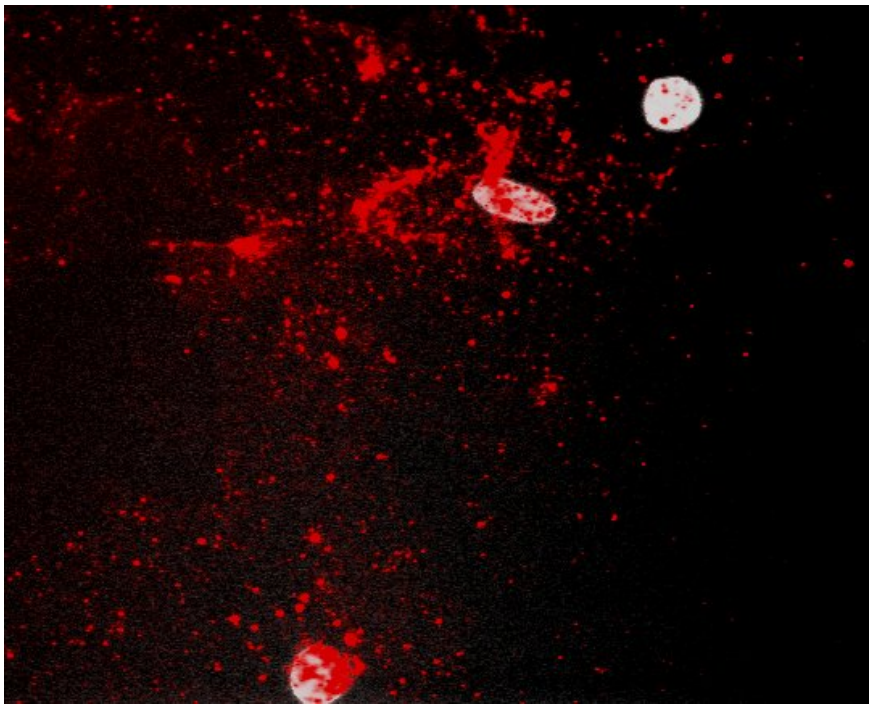

(B)

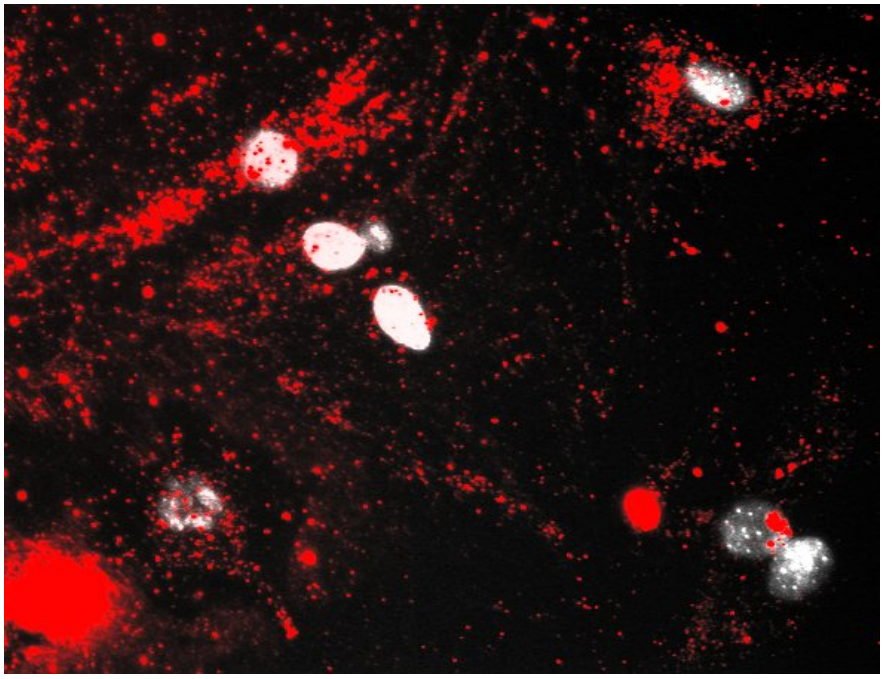

Figure 19: Fluorescence microscopy images of MAE cells 2 hours after beginning treatment. Images of cell nuclei (white) were overlapped with images of the quantum dots (red). (A) MAE caveolin-1 knockout cells (B) MAE wild-type cells treated with targeted quantum dots.

(A)

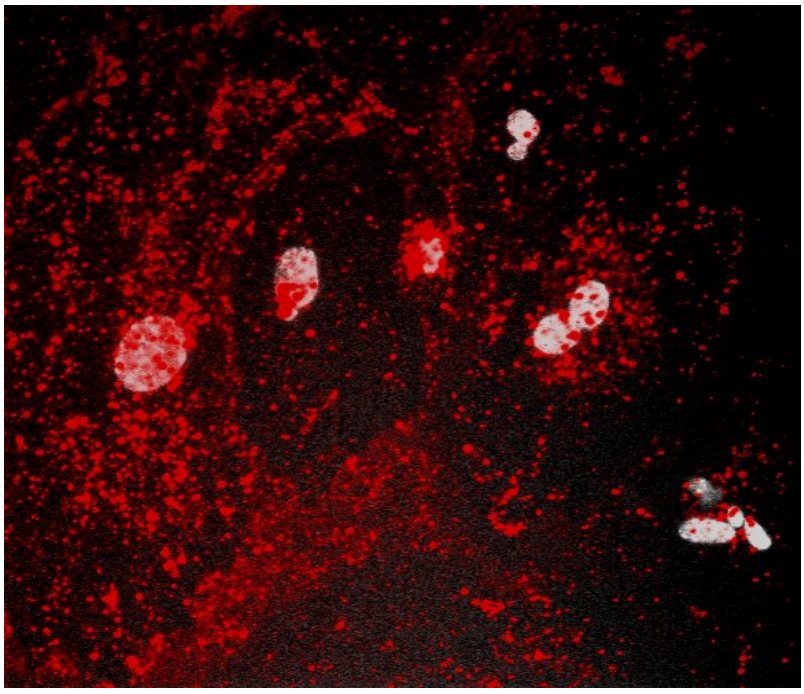

(B)

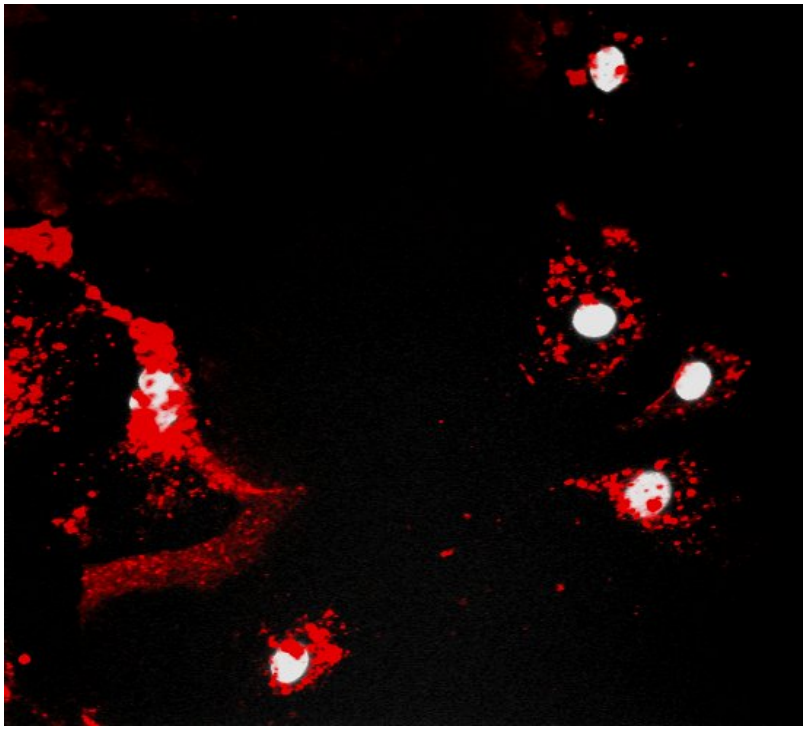

Figure 20: Fluorescence microscopy images of MAE cells 4 hours after beginning treatment. Images of cell nuclei (white) were overlapped with images of the quantum dots (red). (A) MAE caveolin-1 knockout cells (B) MAE wild-type cells treated with targeted quantum dots.

3.4 Effect of Caveolin-1 knockout on the efficacy of uPAR-targeted quantum dots

As done with the MS1 cells, the number of cells remaining after treatment was compared to number at the start of treatment (control). After being treated with free QD and QD-mA, the two groups of cells (wild-type and caveolin-1 knockout) were able to grow and increase in number by ~20%, with the exception of the 5nM treated groups (Figures 21-23). Also, QD and QD-mA treatment did not result in significant differences in the effects on wild-type or caveolin-1 knockout cells with the exception of cells treated with 5nM of QDs in which wild-type cells treated with QD-mA experienced a relatively significant decrease in cell number (Figure 23). At a QD concentration of 5nM, the treatment of wild-type cells with untargeted QDs resulted in a ceasing of cell growth, where as the caveolin-1 knockout cells were able to continue growing (Figure 23). At all concentrations, QD-dox and free dox treatment resulted in a decrease in cell numbers in comparison to the control. However, this effect was more pronounced in wild-type cells (Figures 21-23). Finally as expected, QD-mA-dox treatment resulted in more cell death than both free dox and QD-dox treatment (Figures 21-23). However, its efficacy in causing cell death was significantly decreased in caveolin-1 knockout cells, especially at the 5nM concentration (Figure 21). Again, all of the compounds possessed strong dose-dependant cytotoxic activity.

(A)

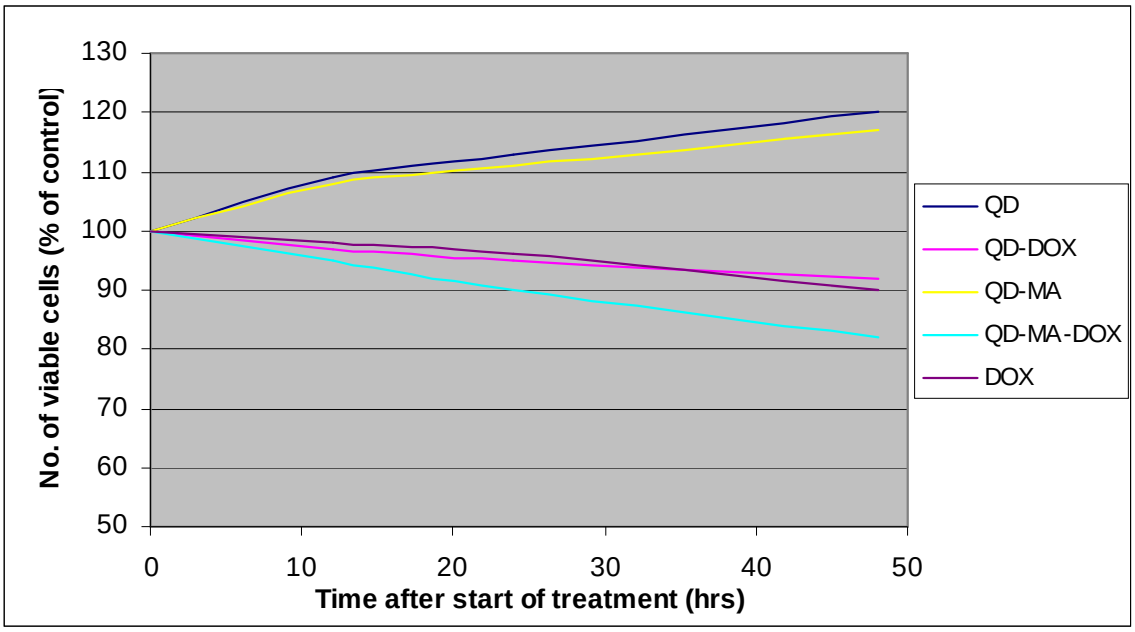

(B)

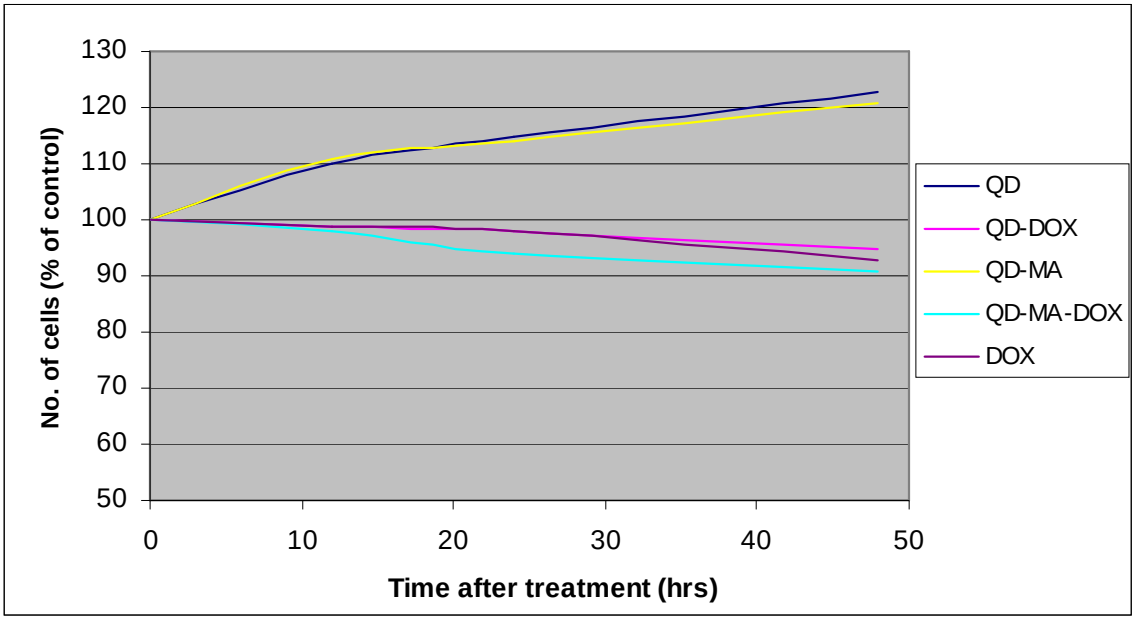

Figure 21: MAE cells were treated with different combinations of quantum dots and free doxorubicin. The percent of cells remaining after 12, 24, and 48 hours post-treatment is compared to the number of cells at the start of treatment. (A) Percent of wild-type cells (B) caveolin-1 knockout cells remaining after treatment with 1nM concentration of quantum dots (500nM free doxorubicin equivalent).

(A)

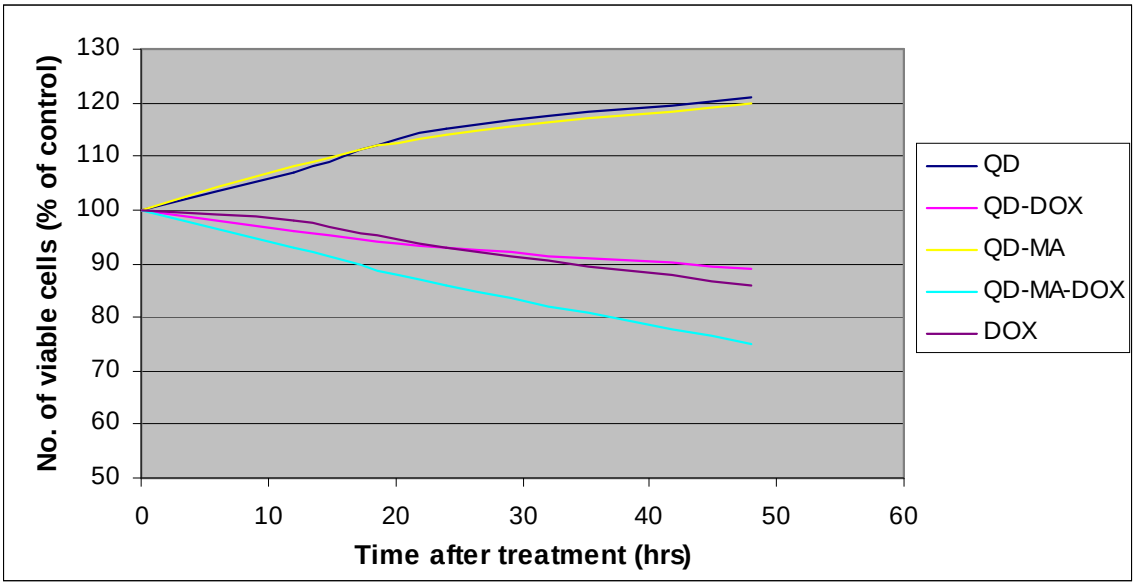

(B)

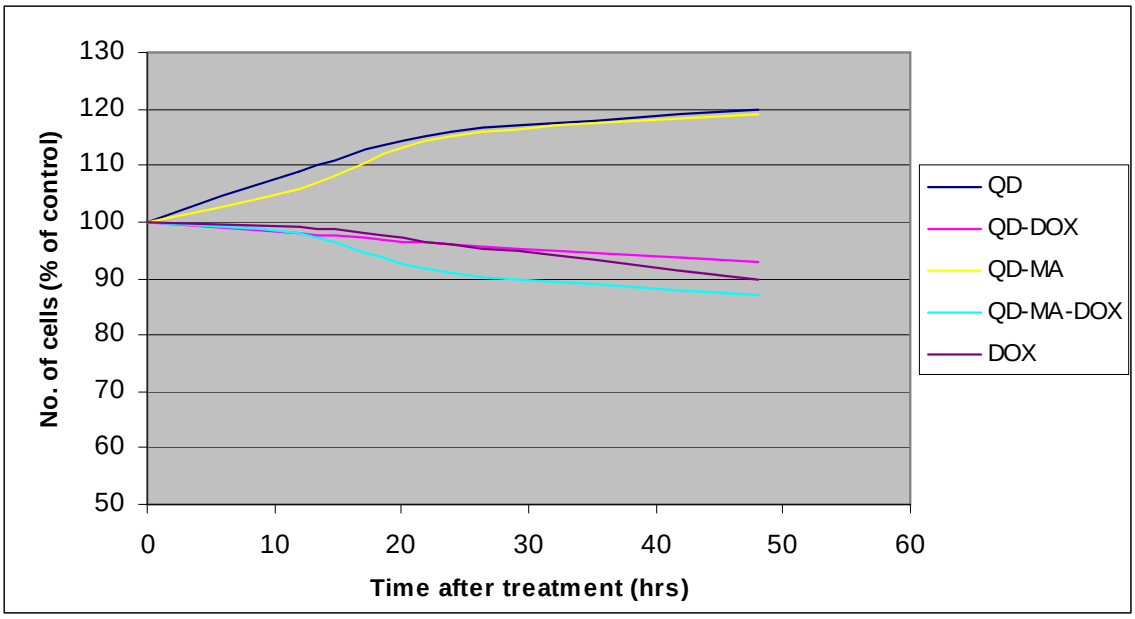

Figure 22: MAE cells were treated with different combinations of quantum dots and free doxorubicin. The percent of cells remaining after 12, 24, and 48hrs post treatment is compared to the number of cells at the start of treatment. (A) Percent of wild-type cells (B) caveolin-1 knockout cells remaining after treatment with 3nM concentration of quantum dots (1.5uM free doxorubicin equivalent).

(A)

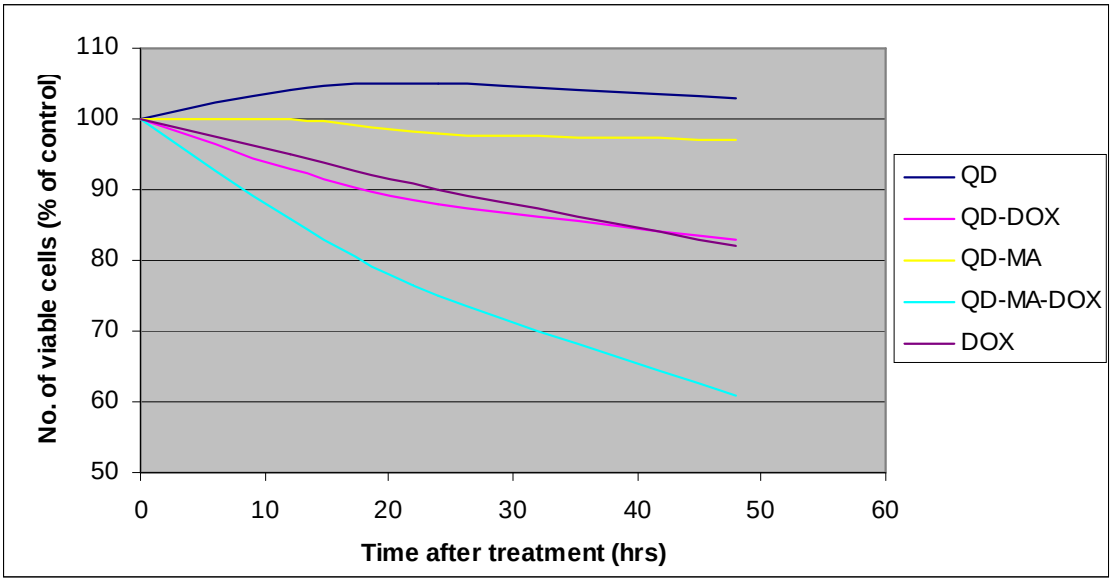

(B)

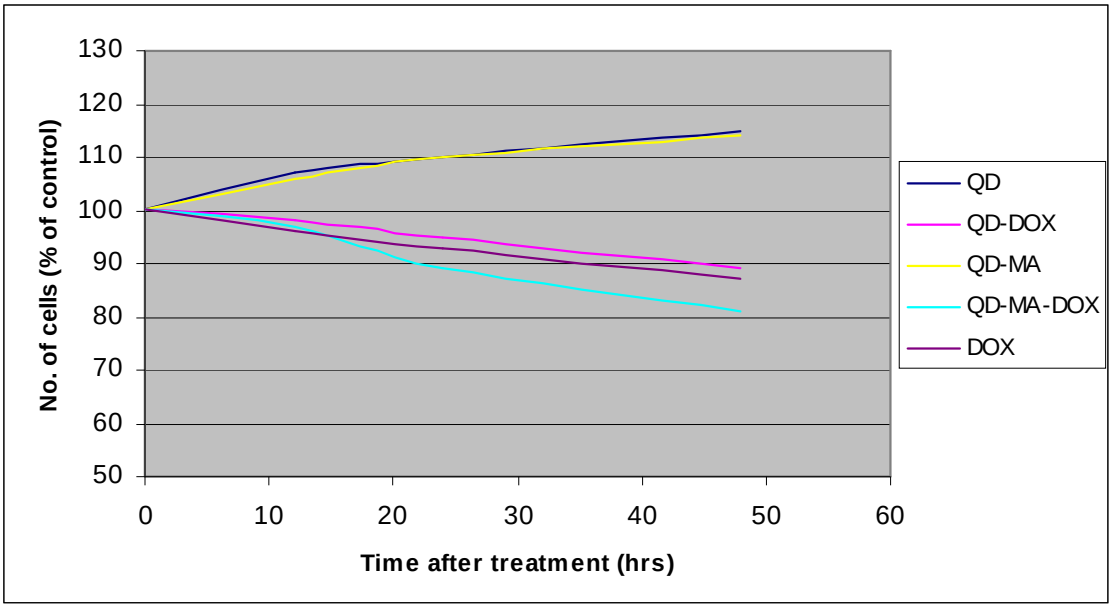

Figure 23: MAE cells were treated with different combinations of quantum dots and free doxorubicin. The percent of cells remaining after 12, 24, and 48hrs post treatment is compared to the number of cells at the start of treatment. (A) Percent of wild-type cells (B)caveolin-1 knockout cells remaining after treatment with 5nM concentration of quantum dots (2.5uM free doxorubicin equivalent).

3.5 Quantification of QD and doxorubicin accumulation within cells

The amount of QDs and doxorubicin in each well was determined using a spectrophotometer. As expected with the above results, uPAR-targeted QDs accumulated within cells more than the untargeted QDs (Figure 24). It is also seen that caveolin-1 knockout cells contained only approximately half the number of quantum dots as compared to the wild-type cells (Figure 24). MAE (wild-type and caveolin-1 knockout) cells contained less targeted and untargeted quantum dots than MS1 cells (Figure 24)

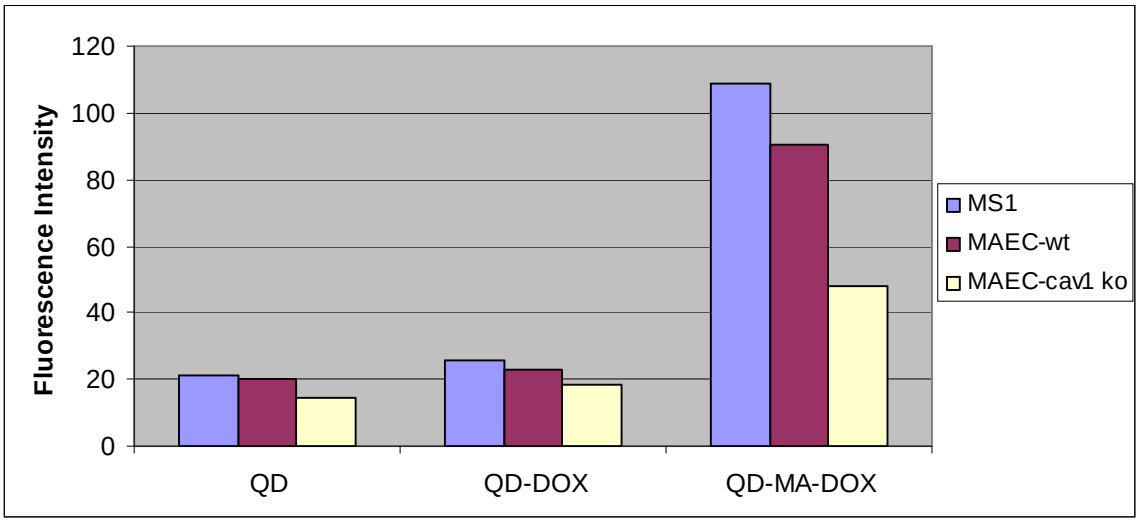

Figure 24: The relative amount of quantum dots was quantified using spectrometry (emission at 620nm). Graph shows the relative fluorescence intensity of quantum dots in each treatment group for each of the three different cell lines.

Doxorubicin levels within each of the cell types corresponded with the levels of quantum dots as show in Figure 24. Cells treated with targeted quantum dots had almost a four-fold increase in intracellular doxorubicin levels compared to unconjugated QDs (Figure 25). As expected by the above results, caveolin-1 knockout cells had much lower levels of doxorubicin compared to the wild-type (Figure 25). Interestingly, free

doxorubicin treated cells had slightly more doxorubicin than QD-dox treated cells (Figure 25).

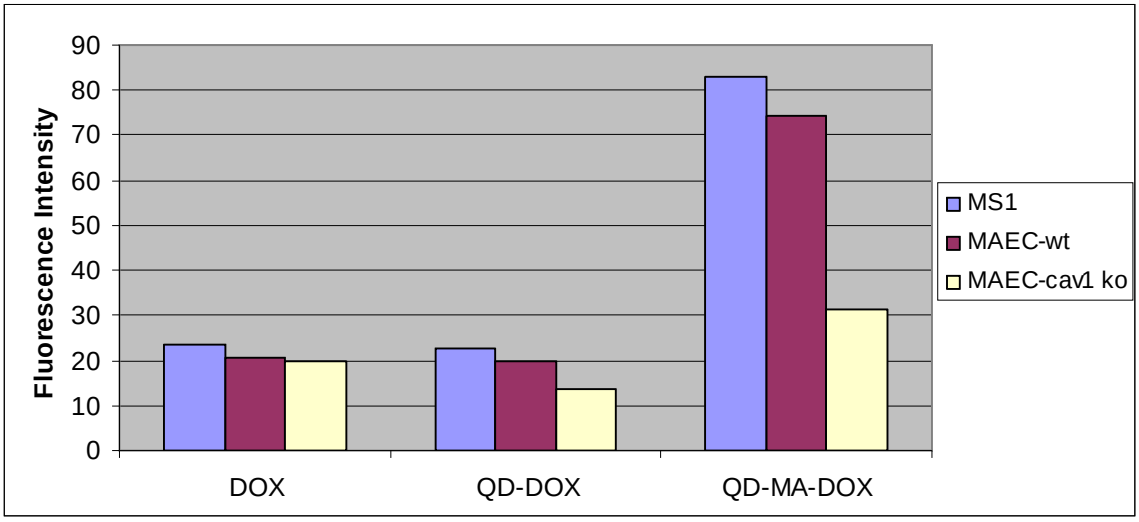

Figure 25: The relative amount of doxorubicin was quantified using spectrometry (emission at 560nm). Graph shows the relative fluorescence intensity of doxorubicin in each treatment group for each of the three different cell lines.

DISCUSSION

Targeted imaging and treatment through the use of nanoparticles holds great promise in improving the survival of patients with cancer. Nanoparticles, due to their small size, are able to pass through the leaky vasculature of tumors and can be modified to allow for multi-modality use. uPAR, which is a receptor that is upregulated in many cancers, is a viable target for ligand conjugated nanoparticles to treat breast and pancreatic cancers among others.

In this thesis, it was investigated whether uPAR-targeted quantum dots were able to accumulate within cells more effectively than their unconjugated counterparts. The accumulation of quantum dots was not only monitored visually using fluorescence microscopy, but also quantified using spectroscopy. Data from these two methods clearly showed the preferential accumulation of targeted quantum dots. Cell counts at various time points also demonstrated the enhanced cytotoxic effects of targeted QDs when compared to both unconjugated QDs and the free drug. As many types of cancers overexpress uPAR, these targeted nanoparticles offer a method of selectively targeting chemotherapeutics to cancer cells.

The mechanism by which uPAR-mediated endocytosis occurs was also elucidated. By comparing the levels of conjugated and unconjugated QDs in wild-type and caveolin-1 knockout cells, it was determined that caveolin-1 is important in the uptake of all forms of quantum dots, although more important for targeted QDs. QDs were not able to as effectively enter caveolin-1 knockout cells as shown using fluorescence microscopy and spectroscopy. Cell counts also confirmed this result by demonstrating that QDs were not

as effective on caveolin-1 knockout cells as they were in the wild-type cells. These results suggest that caveolin plays a major role in uPAR-mediated endocytosis.

4.1 Increased intracellular accumulation of uPAR targeted quantum dots

uPAR targeted quantum dots readily accumulated within cells, and accounted for a 3-4 fold increase in the number of quantum dots compared their untargeted counterparts. It is also noticeable that targeted quantum dots preferentially accumulated within cells around the nuclei. The localization of the quantum dots in this area makes therapy even more effective as the chemotherapeutic agent can be released within the vicinity of the nucleus which is its site of action. Unconjugated quantum dots were also able to accumulate around the nucleus, although this process took much longer. Therefore, targeted chemotherapy is not only more effective because of the increase in effective drug concentration, but also due to the reduction in the time required for drug release, and consequently cell death.

Though the cells used in this study are not cancer cells, the data was able to demonstrate that the efficiency of targeted QDs is dependant on the number of uPAR on the cell surface. As MS1 is a transformed cell line it has a relatively high number of receptors when compared to normal cell lines such as MAEC. This accounts for the difference in targeted QD accumulation within MS1 and MAE cells. However, many cancer cells such as MDA-MB-231 have approximately 300,000 receptors per cell, much higher than the number found on MS1 cells. As normal cells have ~2500 receptors per cell, MDA-MB-231 cells have more than a 100-fold increase in uPAR numbers (Li et al., 1999). Therefore, QDs will accumulate within cancer cells at a much greater efficiency

that it did in MS1 cells even though MS1 cells still demonstrated a strong targeting effect. Targeted therapy will also be more effective in cancer cells as the intercellular environment is more acidic. As doxorubicin is released from the polymer of the QDs by being protonated, this process will occur much more efficiently in cancer cells.

4.2 Effects of quantum dots on cells

As previously mentioned, untargeted quantum dots without doxorubicin was able not only cease cell growth, but also resulted in a decrease in cell number at the 5nM concentration. As quantum dots are composed of cadmium and selenium, it can be imagined that there can be cytotoxic effects. Although the QDs are coated with an amphiphilic polymer, this coating may either not be very effective in protecting the cell from the core's toxicity, or the coating is removed intracellularly. Cadmium is a known carcinogen, and can cause a variety of diseases (Joseph, 2009). Cadmium exerts its toxic effects by binding to the sulfur groups of proteins, therefore inhibiting their function (Helbig, Grosse, & Nies, 2008). Also as cadmium is a divalent ion, it can mimic ions such as calcium. This results in cadmium accumulation within bones, as well as its binding to Ca^{2+} binding proteins (Ohtani-Kaneko et al., 2008). These proteins are vital in a multitude of pathways, therefore explaining cadmium's widespread toxicity. However, this may not be the only mechanism of QD toxicity. As previously shown, QDs accumulate around the nucleus. Though it is difficult to ascertain whether some quantum dots are within the nucleus or in the cytoplasm above the nucleus using fluorescence microscopy, it is not unexpected that QDs can enter the nucleus as they are smaller than the size of nuclear pores. Once within the nucleus, it can not only bind and disrupt enzymes vital for transcription, translation, and the maintenance of DNA (such as repair

machinery), but it can also associate with the negative backbone of DNA due to its positive charge, possibly not only disrupting enzyme activity on DNA but also altering its topology (Joseph, 2009). Finally, QDs can be hypothesized to impair cell growth simply due to its accumulation around the nucleus. The QDs can aggregate and block the nuclear pores, therefore inhibiting vital cellular processes such as the movement of mRNA. While QDs can provide key insights into the mechanism and efficacy of targeted nanoparticles, it is unlikely that they will be used clinically to detect and treat cancers in humans.

4.3 uPAR internalization via caveolin-mediated endocytosis

uPAR-targeted QDs were able to accumulate in MAE (wild-type and caveolin-1 knockout) cells more effectively than untargeted QDs. However, it is seen that caveolin-1 knockout cells do not internalize QDs (conjugated or unconjugated) as effectively as the wild-type cells. This implies that caveolin-1 is important in both uPAR-mediated and non-receptor mediated endocytosis. However, this knockout does not prevent all targeted QDs to enter the cells. Therefore, uPAR can also be internalized via a non-caveolin mediated mechanism. One other known mechanism of uPAR internalization is through a clathrin-mediated process, in which it is internalized in clathrin coated vesicles (Stahl & Mueller, 1995). Future studies will need to investigate the effect of a clathrin knockout on the internalization of uPAR-targeted QDs in order to determine which pathway is the primary mechanism by which uPAR enters the cell.

MS1 cells demonstrated the effect of uPAR-targeted nanoparticles on endothelial cells, therefore elucidating the efficacy of ATF conjugated nanoparticles on not only tumor cells, but also on tumor endothelium. As caveolae are particularly abundant in

vascular endothelia, the binding of ATF conjugated nanoparticles to uPAR (which is also abundant on tumor endothelial cells) may facilitate nanoparticle transport across the endothelium by caveolae-mediated transcytosis. This will allow nanoparticles to rapidly enter into perivascular tumor areas, therefore resulting in the retention and accumulation of nanoparticles in the tumor.

However, it has been shown that caveolin-1 is downregulated in some tumor cells. Further studies will need to demonstrate the role of caveolin-1 in mediating uPAR-targeted nanoparticle endocytosis in those cells in addition to the effects of this downregulation on nanoparticle efficacy. Nonetheless, the determination of the role of caveolin-1 on endothelial cells is significant in understanding the mechanism and efficacy of uPAR-targeted drug delivery on tumor endothelium.

CONCLUSION

In summary, this thesis demonstrates that uPAR-targeted quantum dots are effectively internalized into cells, and exert a greater cytotoxic effect than non-targeted quantum dots. It is also shown that these internalized QDs accumulate around, and in the nucleus, therefore allowing it to release the chemotherapeutic agent near its site of action. Finally, this thesis elucidates the importance of caveolin-1 on the internalization of both targeted and untargeted quantum dots. Caveolin-1 plays a major role in mediating uPAR endocytosis even though there are alternate mechanisms by which this may occur.

REFERENCES

Albain, K. S., Belani, C. P., Bonomi, P., O'Byrne, K. J., Schiller, J. H., & Socinski, M. (2006). PIONEER: a phase III randomized trial of paclitaxel poliglumex versus paclitaxel in chemotherapy-naive women with advanced-stage non-small-cell lung cancer and performance status of 2. *Clin Lung Cancer, 7*(6), 417-419.

Alivisatos, A. P., Gu, W., & Larabell, C. (2005). Quantum dots as cellular probes. *Annu Rev Biomed Eng, 7*, 55-76.

Allen, T. M., & Cullis, P. R. (2004). Drug delivery systems: entering the mainstream. *Science, 303*(5665), 1818-1822.

Atri, M. (2006). New technologies and directed agents for applications of cancer imaging. *J Clin Oncol, 24*(20), 3299-3308.

Barua, S., & Rege, K. (2009). Cancer-cell-phenotype-dependent differential intracellular trafficking of unconjugated quantum dots. *Small, 5*(3), 370-376.

Blasi, F., & Carmeliet, P. (2002). uPAR: a versatile signalling orchestrator. *Nat Rev Mol Cell Biol, 3*(12), 932-943.

Cai, W., Shin, D. W., Chen, K., Gheysens, O., Cao, Q., Wang, S. X., et al. (2006). Peptide-labeled near-infrared quantum dots for imaging tumor vasculature in living subjects. *Nano Lett, 6*(4), 669-676.

Carmeliet, P. (2005). VEGF as a key mediator of angiogenesis in cancer. *Oncology, 69 Suppl 3*, 4-10.

Chan, W. C., & Nie, S. (1998). Quantum dot bioconjugates for ultrasensitive nonisotopic detection. *Science, 281*(5385), 2016-2018.

Cuenca, A. G., Jiang, H., Hochwald, S. N., Delano, M., Cance, W. G., & Grobmyer, S. R. (2006). Emerging implications of nanotechnology on cancer diagnostics and therapeutics. *Cancer, 107*(3), 459-466.

Deryugina, E. I., & Quigley, J. P. (2006). Matrix metalloproteinases and tumor metastasis. *Cancer Metastasis Rev, 25*(1), 9-34.

Fassas, A., & Anagnostopoulos, A. (2005). The use of liposomal daunorubicin (DaunoXome) in acute myeloid leukemia. *Leuk Lymphoma, 46*(6), 795-802.

Fornari, F. A., Randolph, J. K., Yalowich, J. C., Ritke, M. K., & Gewirtz, D. A. (1994). Interference by doxorubicin with DNA unwinding in MCF-7 breast tumor cells. *Mol Pharmacol, 45*(4), 649-656.

Gambhir, S. S. (2002). Molecular imaging of cancer with positron emission tomography. *Nat Rev Cancer, 2*(9), 683-693.

Gao, X., Cui, Y., Levenson, R. M., Chung, L. W., & Nie, S. (2004). In vivo cancer targeting and imaging with semiconductor quantum dots. *Nat Biotechnol, 22*(8), 969-976.

Gao, X., Yang, L., Petros, J. A., Marshall, F. F., Simons, J. W., & Nie, S. (2005). In vivo molecular and cellular imaging with quantum dots. *Curr Opin Biotechnol, 16*(1), 63-72.

Gradishar, W. J. (2005). Albumin-bound nanoparticle paclitaxel. *Clin Adv Hematol Oncol, 3*(5), 348-349.

Hailstones, D., Sleer, L. S., Parton, R. G., & Stanley, K. K. (1998). Regulation of caveolin and caveolae by cholesterol in MDCK cells. *J Lipid Res, 39*(2), 369-379.

Hamm, B., Staks, T., Taupitz, M., Maibauer, R., Speidel, A., Huppertz, A., et al. (1994). Contrast-enhanced MR imaging of liver and spleen: first experience in humans with a new superparamagnetic iron oxide. *J Magn Reson Imaging, 4*(5), 659-668.

Helbig, K., Grosse, C., & Nies, D. H. (2008). Cadmium toxicity in glutathione mutants of Escherichia coli. *J Bacteriol, 190*(15), 5439-5454.

Hofheinz, R. D., Gnad-Vogt, S. U., Beyer, U., & Hochhaus, A. (2005). Liposomal encapsulated anti-cancer drugs. *Anticancer Drugs, 16*(7), 691-707.

Huai, Q., Mazar, A. P., Kuo, A., Parry, G. C., Shaw, D. E., Callahan, J., et al. (2006). Structure of human urokinase plasminogen activator in complex with its receptor. *Science, 311*(5761), 656-659.

Jo, M., Thomas, K. S., Wu, L., & Gonias, S. L. (2003). Soluble urokinase-type plasminogen activator receptor inhibits cancer cell growth and invasion by direct urokinase-independent effects on cell signaling. *J Biol Chem, 278*(47), 46692-46698.

Joseph, P. (2009). Mechanisms of cadmium carcinogenesis. *Toxicol Appl Pharmacol*.

Kjaer, A. (2006). Molecular imaging of cancer using PET and SPECT. *Adv Exp Med Biol, 587*, 277-284.

Kong, G., Anyarambhatla, G., Petros, W. P., Braun, R. D., Colvin, O. M., Needham, D., et al. (2000). Efficacy of liposomes and hyperthermia in a human tumor xenograft model: importance of triggered drug release. *Cancer Res, 60*(24), 6950-6957.

Larocque, J., Bharali, D. J., & Mousa, S. A. (2009). Cancer Detection and Treatment: The Role of Nanomedicines. *Mol Biotechnol*.

Li, Y., Wood, N., Yellowlees, D., & Donnelly, P. K. (1999). Cell surface expression of urokinase receptor in normal mammary epithelial cells and breast cancer cell lines. *Anticancer Res, 19*(2A), 1223-1228.

Mankoff, D. A., Eary, J. F., Link, J. M., Muzi, M., Rajendran, J. G., Spence, A. M., et al. (2007). Tumor-specific positron emission tomography imaging in patients: [18F] fluorodeoxyglucose and beyond. *Clin Cancer Res, 13*(12), 3460-3469.

Mansour, A. M., Drevs, J., Esser, N., Hamada, F. M., Badary, O. A., Unger, C., et al. (2003). A new approach for the treatment of malignant melanoma: enhanced antitumor efficacy of an albumin-binding doxorubicin prodrug that is cleaved by matrix metalloproteinase 2. *Cancer Res, 63*(14), 4062-4066.

Medarova, Z., Pham, W., Farrar, C., Petkova, V., & Moore, A. (2007). In vivo imaging of siRNA delivery and silencing in tumors. *Nat Med, 13*(3), 372-377.

Medina, O. P., Zhu, Y., & Kairemo, K. (2004). Targeted liposomal drug delivery in cancer. *Curr Pharm Des, 10*(24), 2981-2989.

Moghimi, S. M., Hunter, A. C., & Murray, J. C. (2001). Long-circulating and target-specific nanoparticles: theory to practice. *Pharmacol Rev, 53*(2), 283-318.

Moghimi, S. M., & Szebeni, J. (2003). Stealth liposomes and long circulating nanoparticles: critical issues in pharmacokinetics, opsonization and protein-binding properties. *Prog Lipid Res, 42*(6), 463-478.

Moore, A., Weissleder, R., & Bogdanov, A., Jr. (1997). Uptake of dextran-coated monocrystalline iron oxides in tumor cells and macrophages. *J Magn Reson Imaging, 7*(6), 1140-1145.

Nasongkla, N., Bey, E., Ren, J., Ai, H., Khemtong, C., Guthi, J. S., et al. (2006). Multifunctional polymeric micelles as cancer-targeted, MRI-ultrasensitive drug delivery systems. *Nano Lett, 6*(11), 2427-2430.

Ohtani-Kaneko, R., Tazawa, H., Yokosuka, M., Yoshida, M., Satoh, M., & Watanabe, C. (2008). Suppressive effects of cadmium on neurons and affected proteins in cultured developing cortical cells. *Toxicology, 253*(1-3), 110-116.

Peer, D., Karp, J. M., Hong, S., Farokhzad, O. C., Margalit, R., & Langer, R. (2007). Nanocarriers as an emerging platform for cancer therapy. *Nat Nanotechnol, 2*(12), 751-760.

Pelicano, H., Martin, D. S., Xu, R. H., & Huang, P. (2006). Glycolysis inhibition for anticancer treatment. *Oncogene, 25*(34), 4633-4646.

Rao, J. S. (2003). Molecular mechanisms of glioma invasiveness: the role of proteases. *Nat Rev Cancer, 3*(7), 489-501.

Rawat, M., Singh, D., Saraf, S., & Saraf, S. (2006). Nanocarriers: promising vehicle for bioactive drugs. *Biol Pharm Bull, 29*(9), 1790-1798.

Senetta, R., Trevisan, E., Ruda, R., Maldi, E., Molinaro, L., Lefranc, F., et al. (2009). Caveolin 1 expression independently predicts shorter survival in oligodendrogliomas. *J Neuropathol Exp Neurol, 68*(4), 425-431.

Stahl, A., & Mueller, B. M. (1995). The urokinase-type plasminogen activator receptor, a GPI-linked protein, is localized in caveolae. *J Cell Biol, 129*(2), 335-344.

Sturge, J., Wienke, D., East, L., Jones, G. E., & Isacke, C. M. (2003). GPI-anchored uPAR requires Endo180 for rapid directional sensing during chemotaxis. *J Cell Biol, 162*(5), 789-794.

Terada, T., Iwai, M., Kawakami, S., Yamashita, F., & Hashida, M. (2006). Novel PEG-matrix metalloproteinase-2 cleavable peptide-lipid containing galactosylated liposomes for hepatocellular carcinoma-selective targeting. *J Control Release, 111*(3), 333-342.

Vasey, P. A., Kaye, S. B., Morrison, R., Twelves, C., Wilson, P., Duncan, R., et al. (1999). Phase I clinical and pharmacokinetic study of PK1 [N-(2-hydroxypropyl)methacrylamide copolymer doxorubicin]: first member of a new class of chemotherapeutic agents-drug-polymer conjugates. Cancer Research Campaign Phase I/II Committee. *Clin Cancer Res, 5*(1), 83-94.

Wei, Y., Yang, X., Liu, Q., Wilkins, J. A., & Chapman, H. A. (1999). A role for caveolin and the urokinase receptor in integrin-mediated adhesion and signaling. *J Cell Biol, 144*(6), 1285-1294.

Weissleder, R. (2006). Molecular imaging in cancer. *Science, 312*(5777), 1168-1171.

Yang, L., Mao, H., Cao, Z., Wang, Y. A., Peng, X., Wang, X., et al. (2009). Molecular Imaging of Pancreatic Cancer in an Animal Model Using Targeted Multifunctional Nanoparticles. *Gastroenterology*.

Yatvin, M. B., Kreutz, W., Horwitz, B. A., & Shinitzky, M. (1980). pH-sensitive liposomes: possible clinical implications. *Science, 210*(4475), 1253-1255.